Ion-Acoustic Anomalous Resistivity: Theory and Observations

Panagiota Petkaki
Physical Sciences Division
British Antarctic Survey
Cambridge, UK

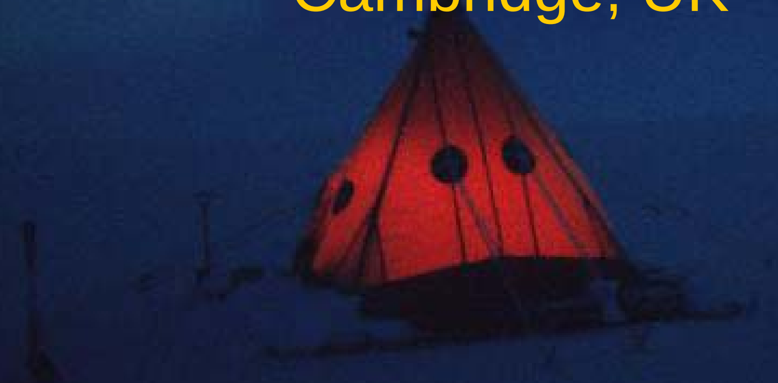

Collaborators

- Mervyn Freeman (BAS)
- Clare Watt (University of Alberta, Canada)
- Richard Horne (BAS)
- Tobias Kirk (University of Cambridge)

Reconnection in Collisionless Plasmas

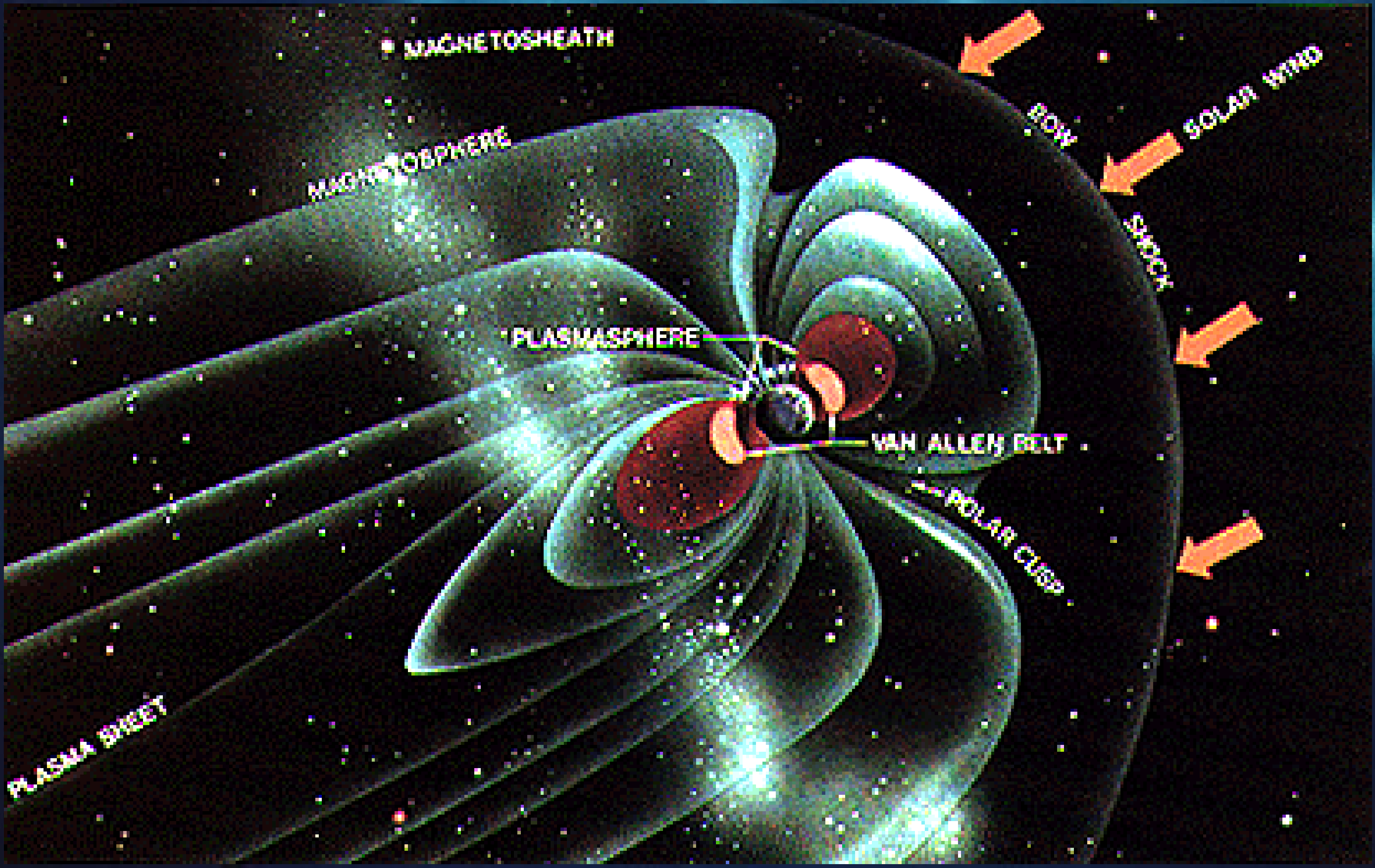

Reconnection and Geospace

- Geospace is the only environment in which reconnection can be observed both
  - In-situ (locally) by spacecraft
  - Remotely from ground (globally)
- Reconnection between interplanetary magnetic field and geomagnetic field at magnetopause
- Drives plasma convection cycle involving reconnection in the magnetotail.
- Courtesy of M. Freeman

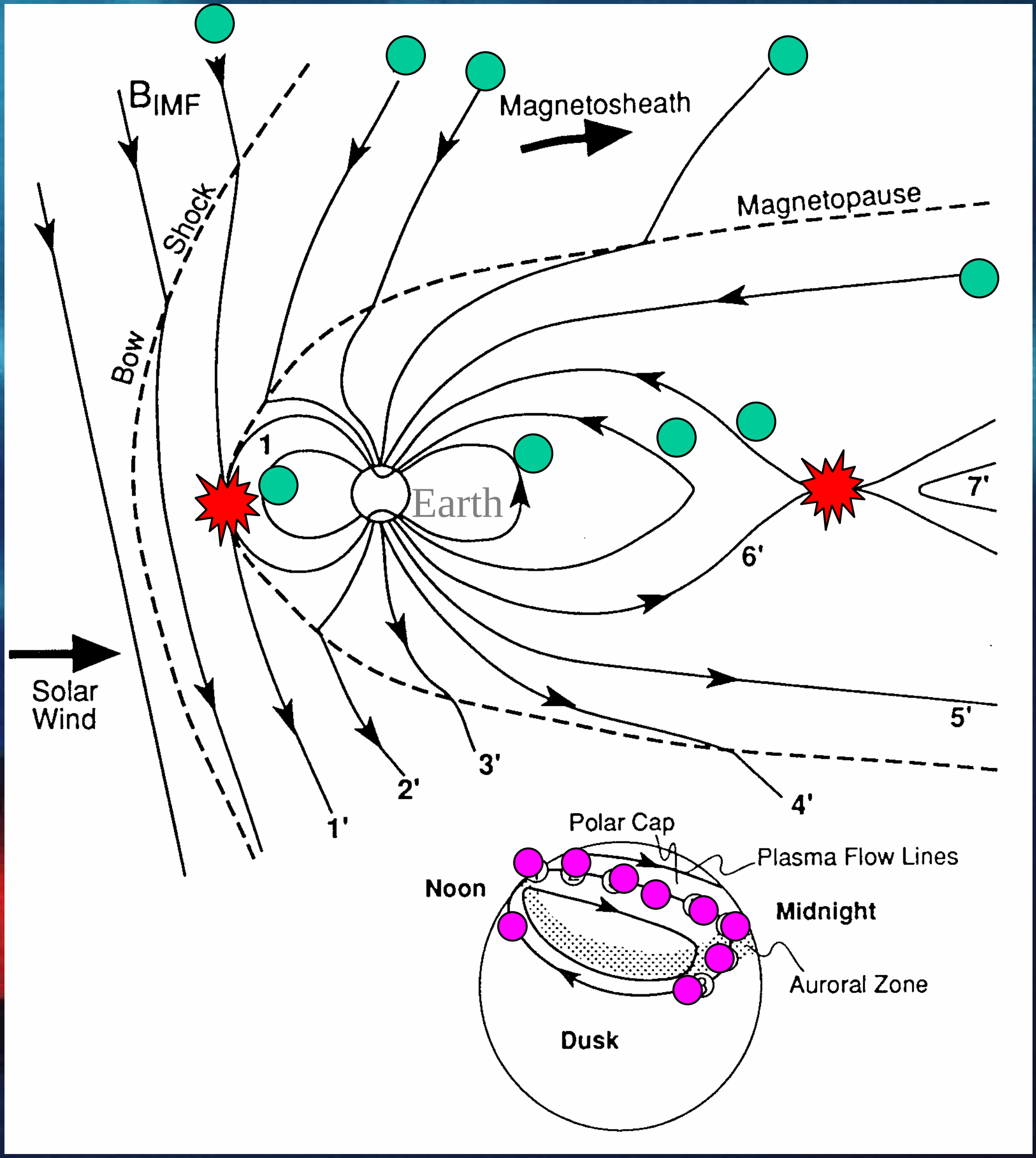

Evidence for reconnection in Earth's magnetosphere

- Dependence of many phenomena on Interplanetary Magnetic Field orientation relative to Earth's magnetic dipole
  - convection strength and pattern
  - auroral activity
- Mixing of solar and terrestrial plasmas
  - energy dispersion and cut-offs
- In-situ observation of X- and O-type magnetic reconnection structures
  - magnetic nulls
  - magnetic islands (plasmoids)
  - bi-directional jets

The Problem

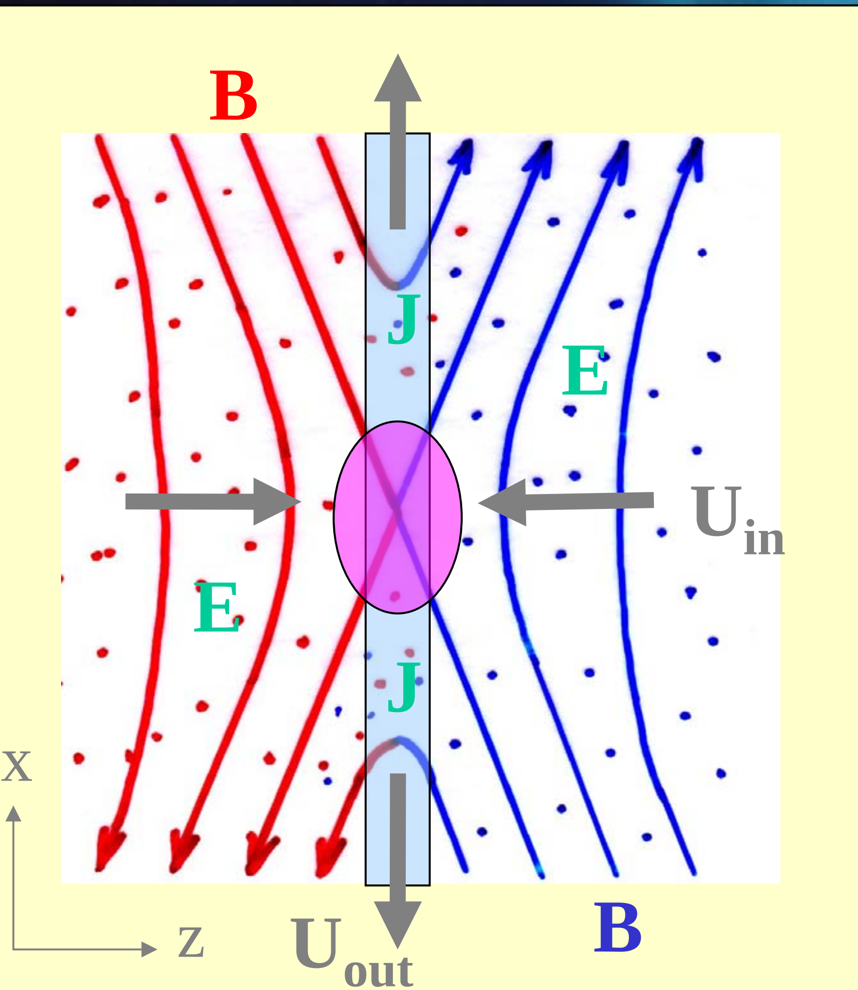

- Reconnection at MHD scale requires violation of frozen-in field condition:

$$\underline{E}+\underline{v}\times\underline{B}=\frac{m_e}{ne^2}\frac{\partial \underline{J}}{\partial t}+\frac{m_e}{ne^2}\left(\underline{v}\,\underline{J}+\underline{J}\,\underline{v}\right)-\frac{1}{ne}\nabla\cdot\underline{\underline{p_e}}+\frac{1}{ne}\left(\underline{J}\times\underline{B}\right)+\frac{m_e}{ne^2}\nu_e\underline{J}$$

- Kinetic-scale wave turbulence can scatter particles to generate anomalous resistivity at MHD scale [Davidson and Gladd, 1975] :

$$\eta=-\frac{1}{\varepsilon_o\omega_{pe}^2 p_e}\frac{\partial p_e}{\partial t}=\frac{1}{\varepsilon_o\omega_{pe}^2 J}\frac{\partial J}{\partial t}$$

- How does anomalous resistivity depend on MHD variables (*n*, *T*,**J**)?

Change in Electron inertia from wave-particle interaction

- Waves could be important in scattering electrons.
- Change in electron momentum p_e contributes to electron inertial term [Davidson and Gladd, 1975]
- Broad band waves seen in crossing of reconnecting current sheet [Bale et al., Geophys. Res. Lett., 2002].
- The Measured Electric Field is more than 100 times the analytically estimated due to Lower Hybrid Drift Instability

$$\eta = \frac{1}{\omega_{pe}\varepsilon_o}\frac{W_E}{nk_BT_e}$$

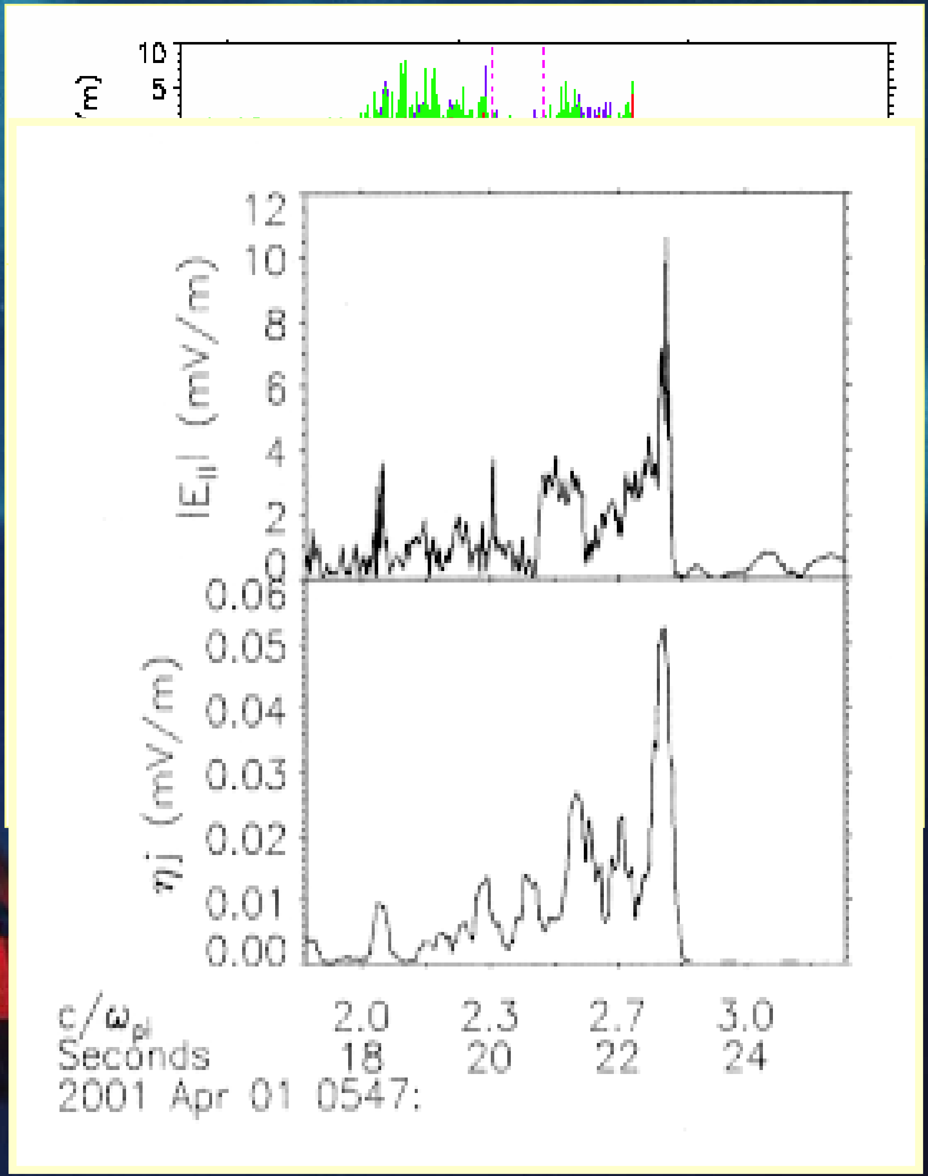

Anomalous Resistivity due to Ion-Acoustic Waves

- 1-D electrostatic Vlasov simulation of resistivity due to ion-acoustic waves.
- *Sagdeev [1967],Labelle and Treumann [1988]* assume $T_e \gg T_i$ which is not the case for most space plasma regions of interest (e.g. magnetopause).
- Resistivity is 1000 times greater than Labelle and Treumann [1988] theoretical (quasi-linear) estimate (depending on realistic mass ratio)
  - must take into account the changes in form of the distribution function.
- Consistent with observations in reconnection layer [Bale et al., Geophys. Res. Lett., 2002]

Watt et al., Geophys. Res. Lett., 2002

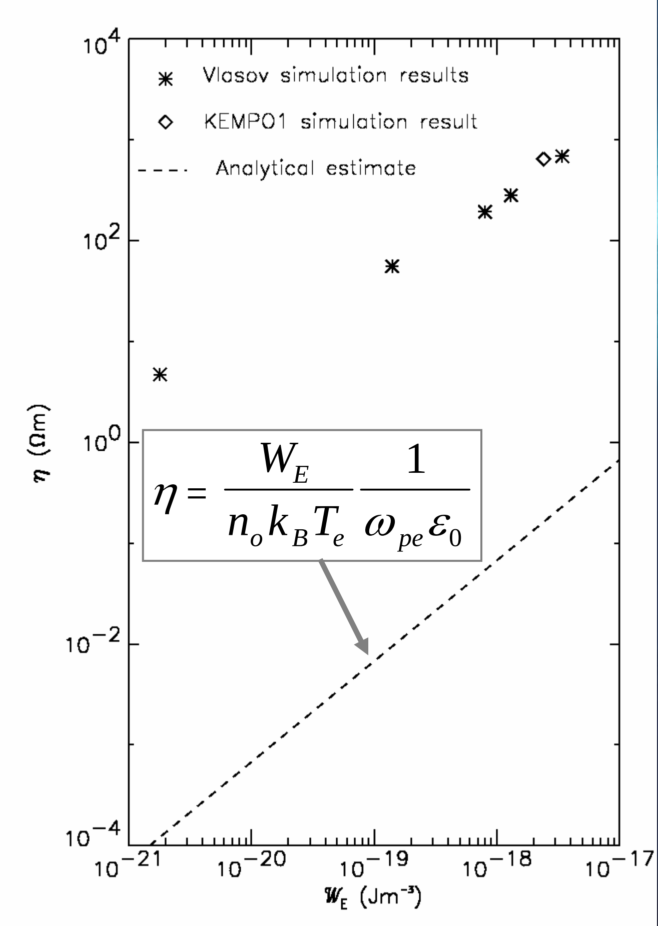

Outline of Seminar

- Why Ion-Acoustic waves
- Vlasov Simulation description
- Ion-Acoustic Resistivity for Lorentzian and Maxwellian Plasma
- Non-linear Evolution of Ion-Acoustic Instability
- Cluster Observations of wave activity

Ion-Acoustic Waves in Space Plasmas

- **Ionosphere, Solar Wind, Earth's Magnetosphere**
- **Natural Modes in Unmagnetised Plasmas**
  - ***driven unstable in no magnetic field and in uniform magnetic field***
- **Centre of Current Sheet - driven unstable by current**
- **Source of diffusion in Reconnection Region**
- **Current-driven Ion-Acoustic Waves – finite drift between electrons and ions**

Evolution of Vlasov Simulation

One-dimensional and electrostatic with periodic boundary conditions.

- **Plasma species α modelled with $f_\alpha(z, v, t)$ on discrete grid**
- **f_α evolves according to Vlasov eq. E evolves according to Ampère's Law**

$$\frac{\partial f_\alpha}{\partial t} = -v_z \frac{\partial f_\alpha}{\partial z} - \left(\frac{q_\alpha}{m_\alpha}\right) E \frac{\partial f_\alpha}{\partial v_z}$$

$$\frac{\partial E}{\partial t} = -\mu_0 c^2 J + \nabla \times \mathbf{B}_{ext}$$

- **In-pairs method**

$$J = \sum_\alpha \int_{-\infty}^{\infty} q_\alpha v f_\alpha \, \mathrm{d}v$$

- **The B = 0 in the current sheet, but curl B = $\mu_0 c^2 J$.**
- **MacCormack method**
- **Resistivity**

$$\eta = -\left(\frac{1}{\omega_{pe}^2 \varepsilon_0}\right) \frac{1}{p_e} \frac{\partial p_e}{\partial t}$$

Finite Difference Equations

Using MacCormack's method the forward finite difference for $(\partial f_{i,j}/\partial t)$ is:

$$\frac{\partial f_{i,j}}{\partial t} = -v_j \left(\frac{f_{(i+1),j}(t) - f_{i,j}(t)}{\Delta z} \right) - \frac{q_\alpha}{m_\alpha} E_i(t) \left(\frac{f_{i,(j+1)}(t) - f_{i,j}(t)}{\Delta v_z} \right) \qquad (4)$$

Use this to predict the DF at the next time step:

$$\overline{f_{i,j}(t+\Delta t)} = f_{i,j}(t) + \Delta t \frac{\partial f_{i,j}}{\partial t} \qquad (5)$$

Use the predicted value of $\overline{f_{i,j}(t+\Delta t)}$ to

rected" time derivative

$$\left(\overline{\frac{\partial f_{i,j}}{\partial t}}\right) = -v_z \left(\frac{\overline{f_{i,j}(t+\Delta t)} - \overline{f_{(i-1),j}(t}}{\Delta z} \right. \quad -\frac{q_\alpha}{m_\alpha} \overline{E_i(t+\Delta t)} \left(\frac{\overline{f_{i,j}(t+\Delta t)} - \overline{f_{i,(j-1)}}}{\Delta v_z} \right.$$

where $\overline{E_i(t+\Delta t)}$ is the value of E_z at the ne

The new value of $f_{i,j}(t+\Delta t)$ is

$$f_{i,j}(t+\Delta t) = f_{i,j} + \frac{\Delta t}{2} \left(\frac{\partial f_{i,j}}{\partial t} + \left(\overline{\frac{\partial}{\partial}} \right. \right.$$

In-pairs integration method [*Horne and Freeman*, 2001].

$$\begin{aligned} n_\alpha(z,t) &= \int_{-\infty}^{\infty} f_\alpha(z, v_z, t)\, dv_z \\ &= \sum_{i=-N_v}^{N_v-1} \frac{1}{2} \left[f_\alpha(z,i,t) + f_\alpha(z,i+1,t) \right] \Delta v_z \quad (8) \end{aligned}$$

$$\begin{aligned} n_\alpha(z,t) &= \left[\frac{1}{2} f_\alpha(z,-N_v,t) + \frac{1}{2} f_\alpha(z,N_v,t) \right] \Delta v_z \\ &+ \left[\sum_{i=-N_v}^{0} \left[f_\alpha(z,i,t) + f_\alpha(z,-i,t) \right] \right] \Delta v_z \quad (9) \end{aligned}$$

Vlasov Simulation Initial Conditions

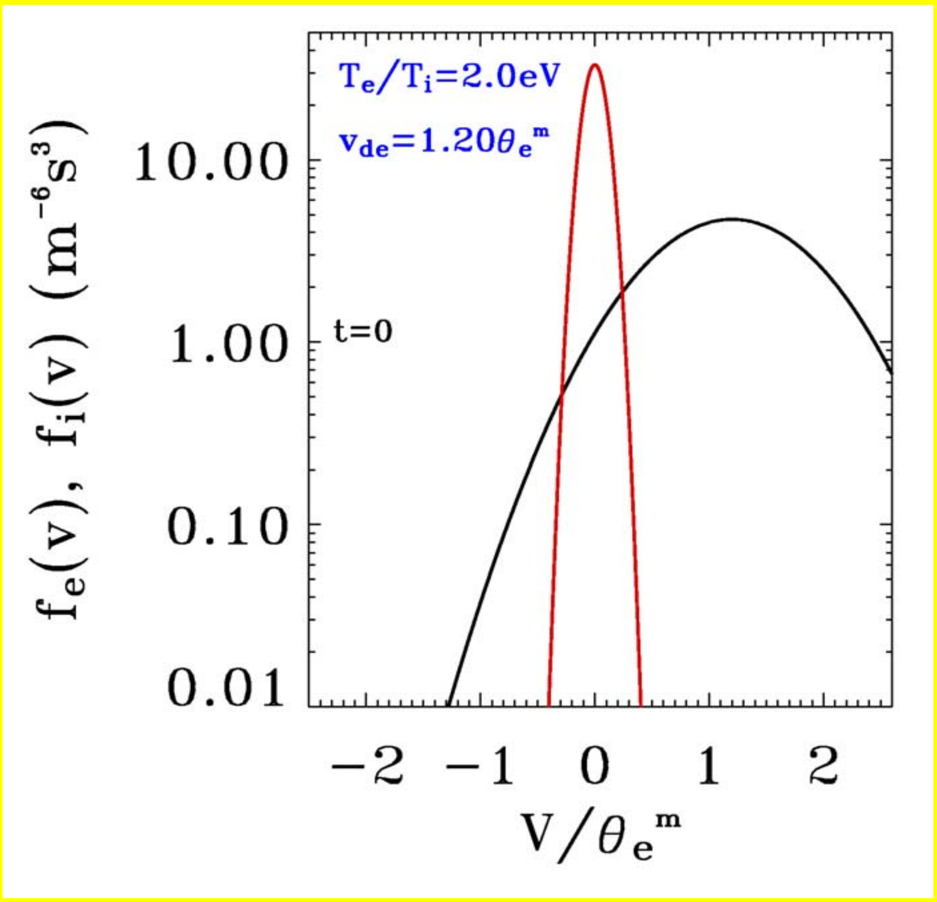

- **CDIAW- drifting electron and ion distributions**
- **Apply white noise Electric field**

$$E_1(z,0) = \sum_{n=1}^{N} E_{tf} \sin\left(k_n z + \varphi\right)$$

$$E_{tf} = \left(\frac{2k_B T_e}{\varepsilon_0 \lambda_{De}^3}\right)^{1/2}$$

- **f_α close to zero at the edges**
- ***Maxwellian***
- **Drift Velocity - V_{de} = 1.2 x θ**
  (θ = $(2T/m)^{1/2}$)
- **M_i=25 m_e**
- **T_i=1 eV, T_e = 2 eV**
- **n_i=n_e = 7 x 10^6 /m^3**
- **N_z = 642, N_{ve} = 891, N_{vi} = 289**

Grid of Vlasov Simulation

Significant feature of the Code : Number of grid points to reflect expected growing wavenumbers - ranges of resonant velocities

- **Spatial Grid : $N_z=L_z/\Delta z$**
  - **Largest Wavelength (Lz)**
  - **Δz is 1/12 or 1/14 of smallest wavelength**
- **Velocity Grid Nv{e,i} =2 X ($v_{cut}/\Delta v\{e,i\}$) +1**
  - **vcut > than the highest phase velocity**
  - **Vcut,e = 6 θ + drift velocity or 12 θ + drift velocity**
  - **Vcut,i = 10 θ or 10 maximum phase velocity**
- **Time resolution**
  - **Courant number**
  - **One velocity grid cell per timestep**

$$\Delta t \le \frac{\Delta z}{vcut}$$

$$\Delta t \le \frac{m_\alpha}{q_\alpha}\frac{\Delta v}{E_{\max}}$$

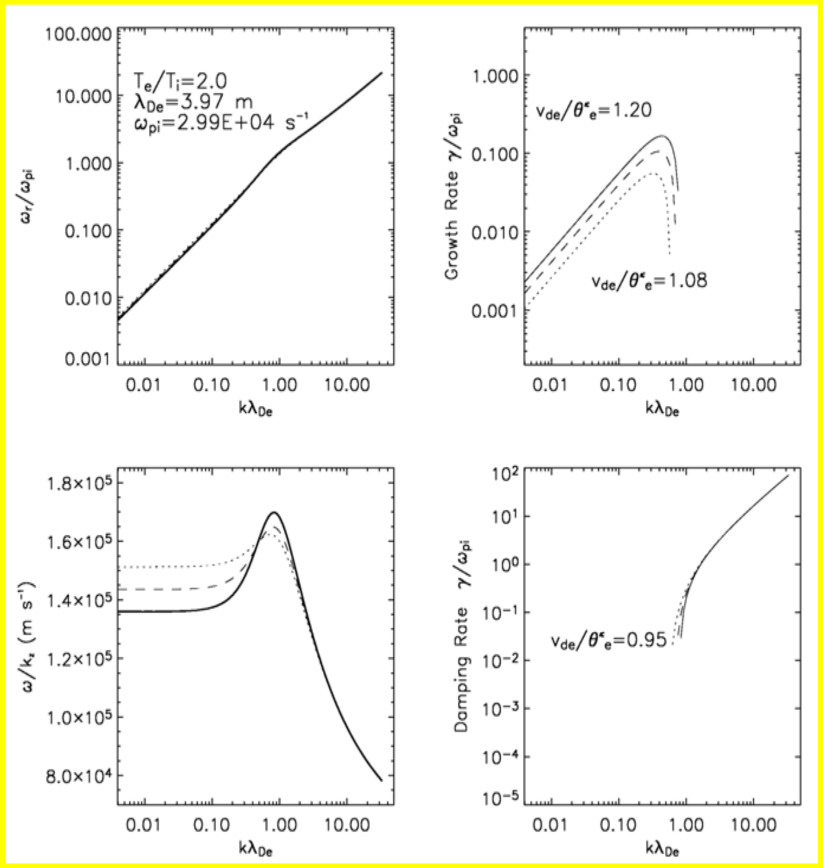

Linear Dispersion Relation

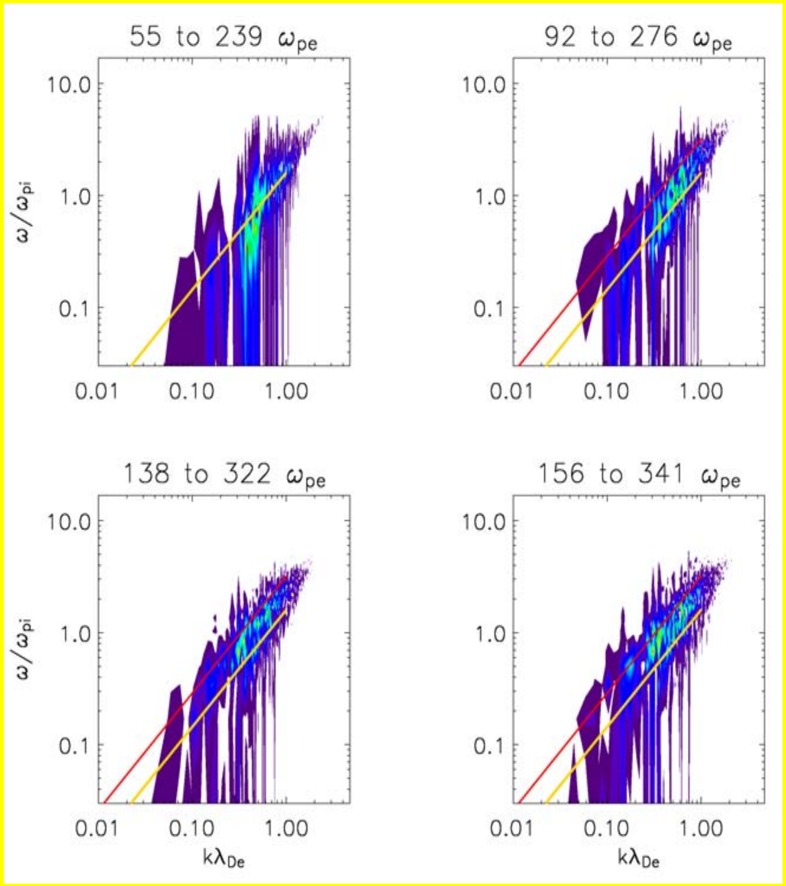

Dispersion Relation from Vlasov Simulation

642 k modes

Maxwellian Run

- Evolution from linear to quasi-linear saturation to nonlinear
- Distribution function changes
- Plateau formation at linear resonance
- Ion distribution tail

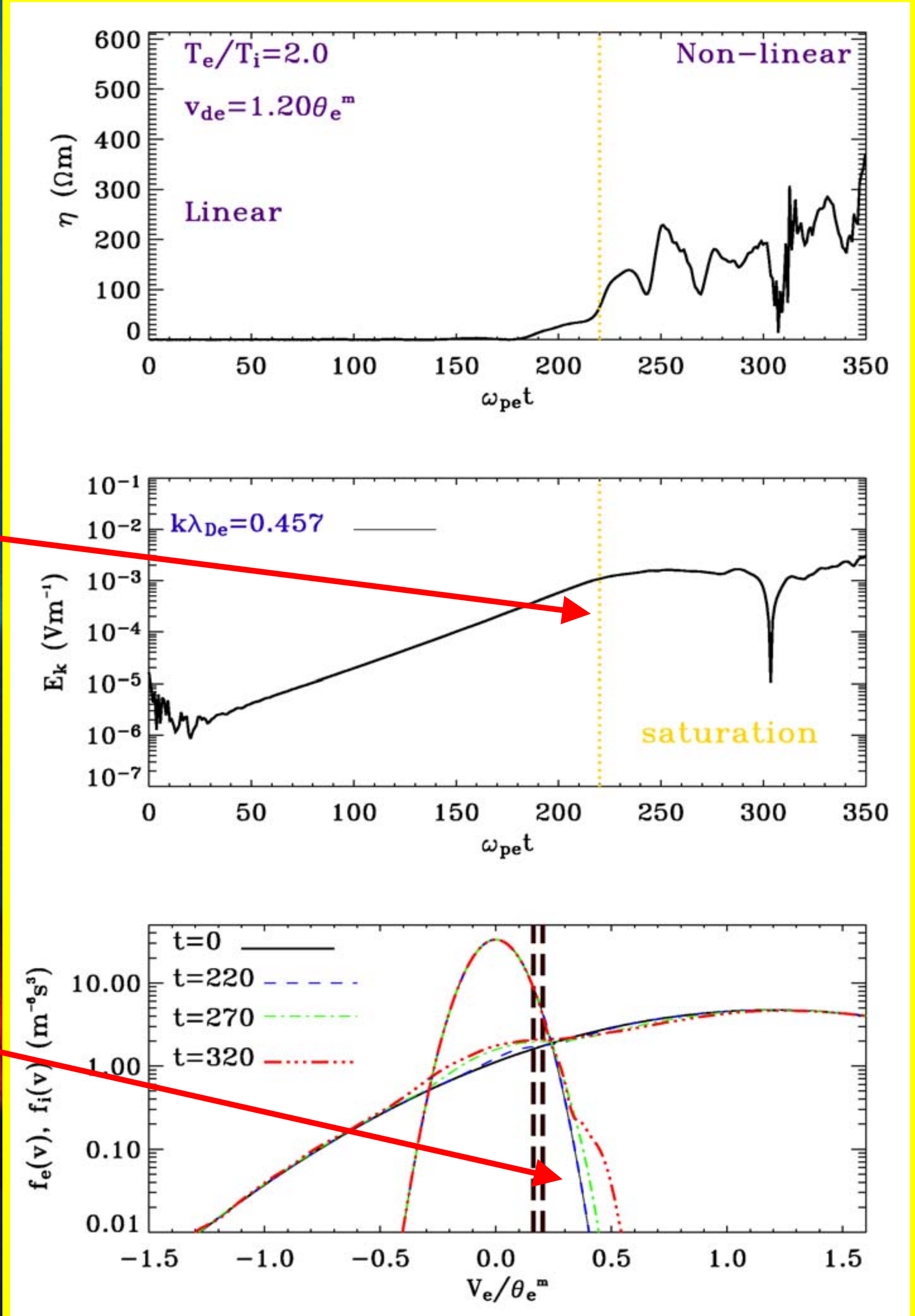

Time-Sequence of Full Electron Distribution Function

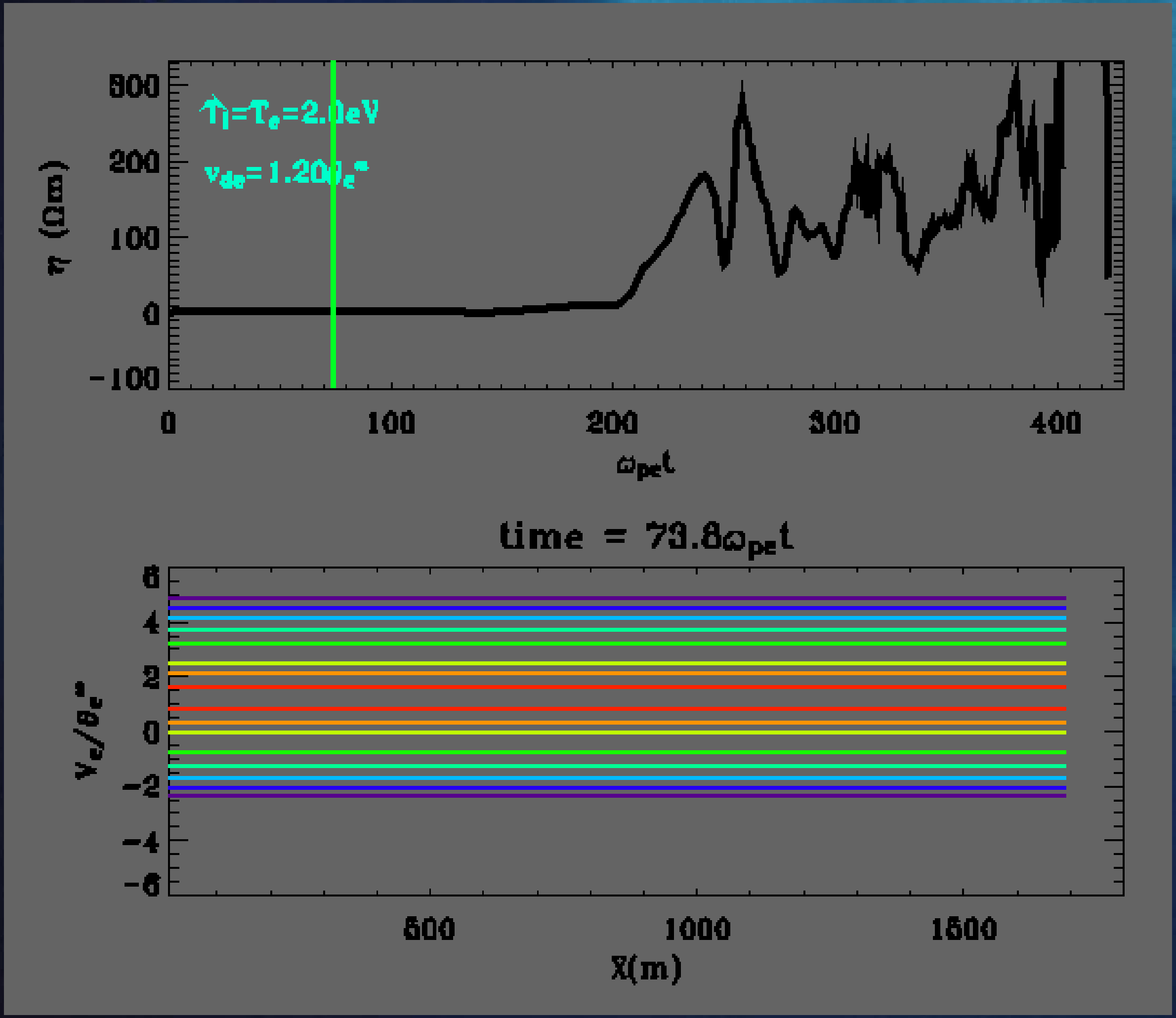

- Top figure : Anomalous resistivity
- Lower figure : Electron DF

Time-Sequence of Full Ion Distribution Function

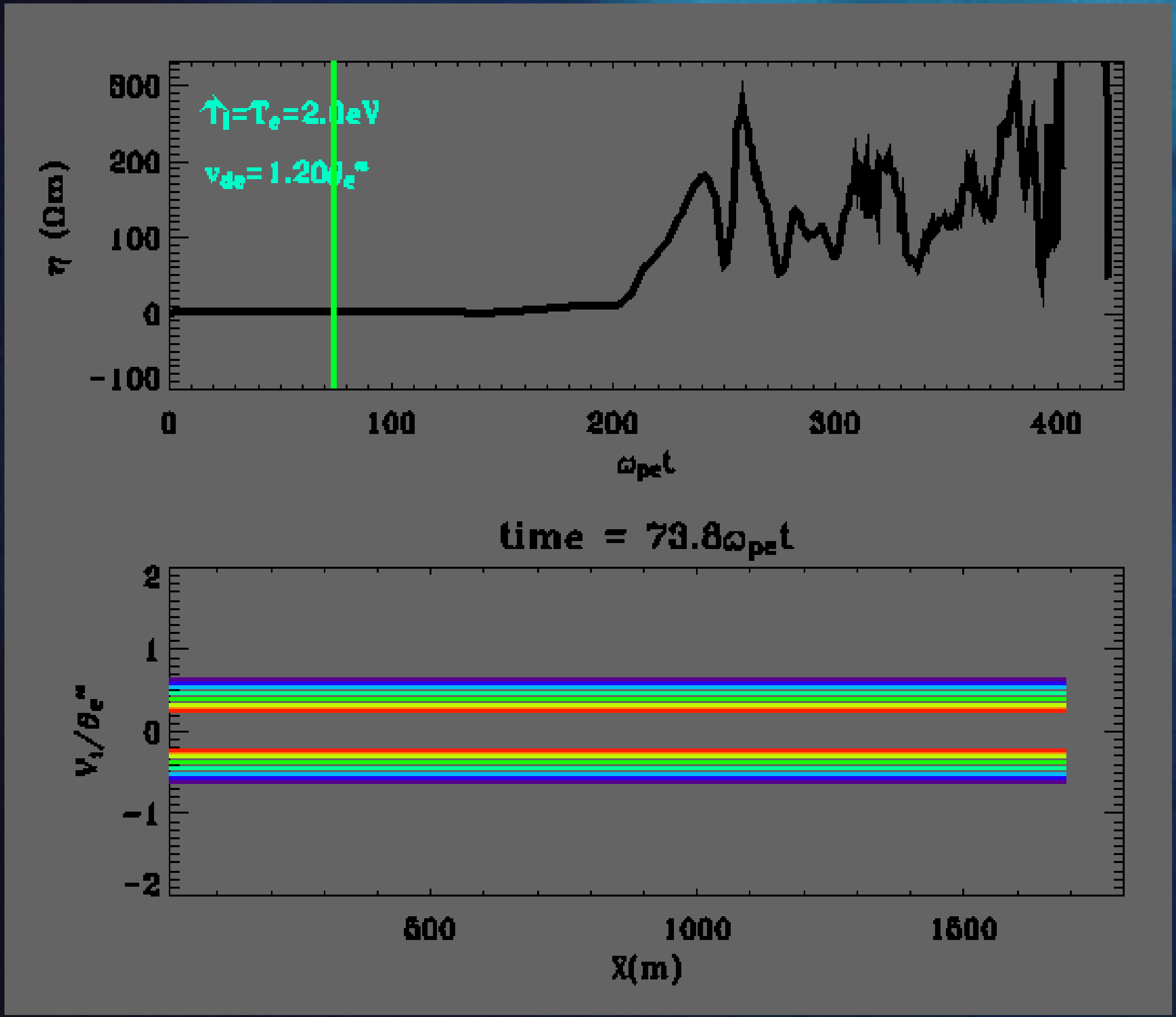

- Top figure : Anomalous resistivity
- Lower figure : Ion DF

Lorentzian Distribution Functions

- **Lorentzian DF : Planetary Magnetospheres, Astrophysical Plasmas, Solar Wind (e.g. Collier, 1999)**
- **Different positive slope of DF at resonant region for instability**
- **Conditions for CDIAW* for κ=2 to 7 altered from Maxwellian DF**

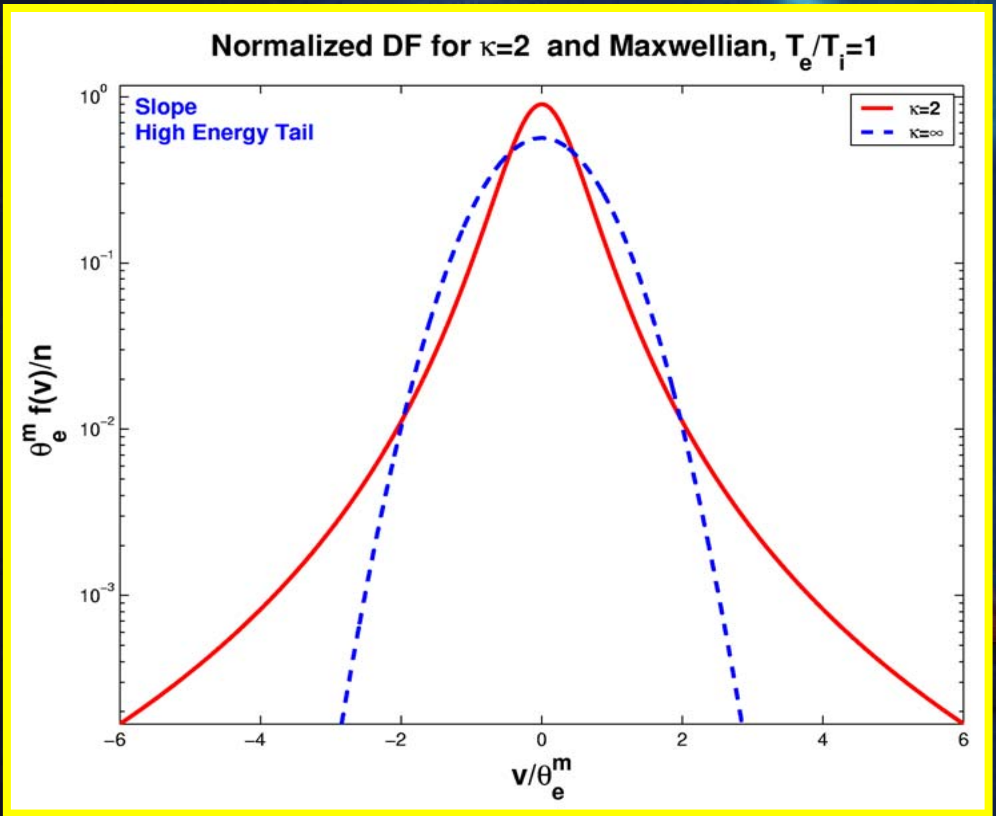

$$f_\kappa(\upsilon) = \frac{N}{\pi^{3/2}} \frac{1}{\theta^3} \times$$

$$\frac{\Gamma(\kappa+1)}{\kappa^{3/2}\Gamma(\kappa - 1/2)} \left(1 + \frac{\upsilon^2}{\kappa\theta^2}\right)^{-(\kappa+1)}$$

* Current Driven Ion-Acoustic Waves

- Summers and Thorne (1991) introduced the modified Plasma Dispersion Function
- Linearise Vlasov Equation using Modified Plasma Dispersion Function and Lorentzian DF to obtain Dispersion Relation of Current-Driven Ion-Acoustic Waves
- Newton-Raphson method to solve Dispersion relation

$$
\begin{aligned}
1 = &-\frac{2\omega_{pe}^2}{k^2\theta_e^2}\left[1-\frac{1}{2\kappa}+\frac{\omega-k\upsilon_{d,e}}{k\theta_e}Z_\kappa^*\left(\frac{\omega-k\upsilon_{d,e}}{k\theta_e}\right)\right] \\
&-\frac{2\omega_{pi}^2}{k^2\theta_i^2}\left[1-\frac{1}{2\kappa}+\frac{\omega-k\upsilon_{d,i}}{k\theta_i}Z_\kappa^*\left(\frac{\omega-k\upsilon_{d,i}}{k\theta_{ie}}\right)\right]
\end{aligned}
$$

Modified Plasma Dispersion Function

- Summers and Thorne (1991) introduced the modified Plasma Dispersion Function

$$Z_\kappa^*(\xi) = \frac{1}{\sqrt{\pi}} \frac{\kappa^{(\kappa-1/2)}\Gamma(\kappa+1)}{\Gamma(\kappa-1/2)} F(\xi)$$

where

$$F(\xi) = \int_{-\infty}^{\infty} \frac{\phi(s)}{(s-\xi)} ds$$

with

$$\phi(s) = (s^2+\kappa)^{-(\kappa+1)}$$

Critical Electron Drift Velocity Normalized to

$$\theta = \left(\frac{\kappa - 3/2}{\kappa} \frac{2k_B T}{m} \right)^{1/2}$$

$M_i = 1836 m_e$

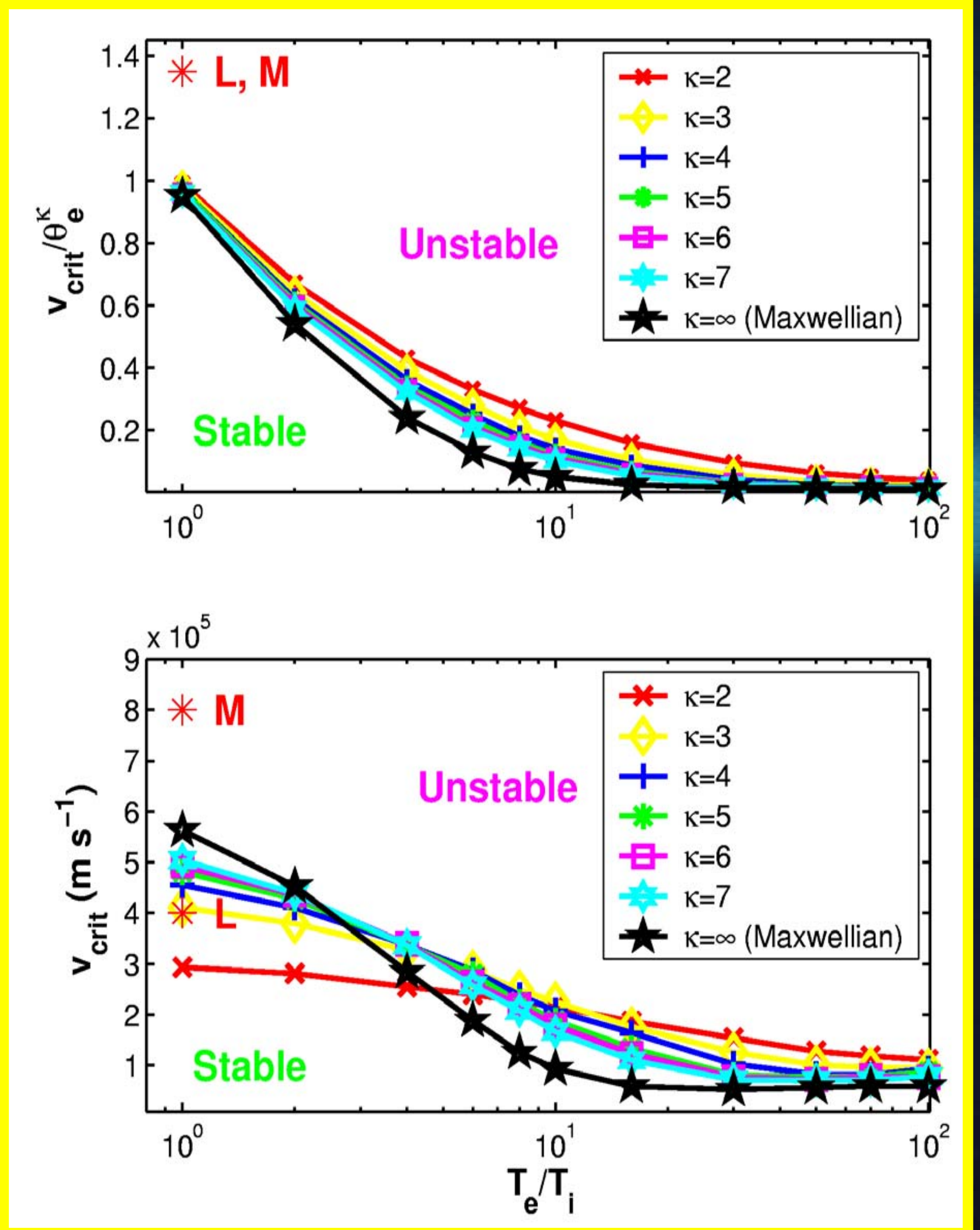

Effect of the reduced mass ratio on the stability curves.

The Maxwellian case is plotted as κ = 80 for illustration purposes.

Curves are plotted for

T_e / T_i = 1.

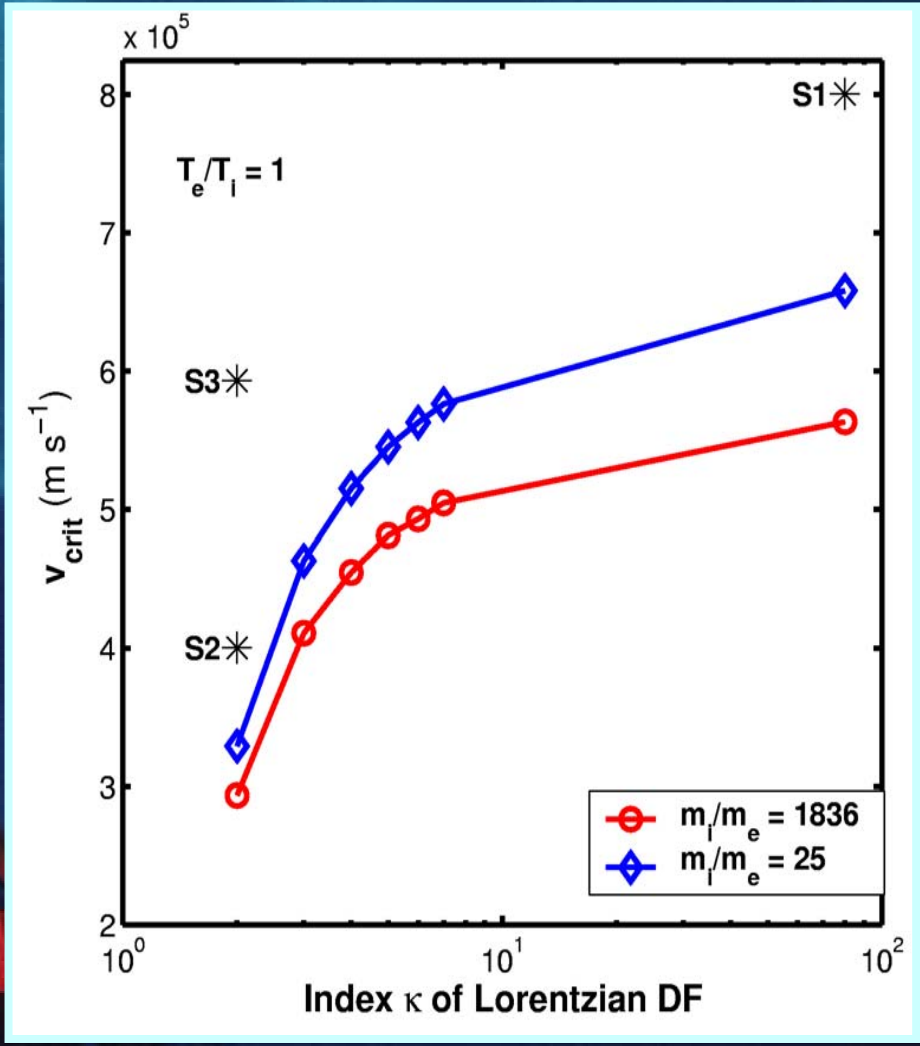

Compare Anomalous Resistivity from Three Simulations

- **S1 - Maxwellian –**
  $V_{de} = 1.35 \times \theta \; (\theta = (2T/m)^{1/2})$
  Nz=547, Nve=1893, Nvi=227
- **S2 - Lorentzian -**
  $V_{de} = 1.35 \times \theta$
  $(\theta = [(2\kappa-3)/2\kappa]^{1/2} (2T/m)^{1/2})$
  Nz=593, Nve=2667, Nvi=213
- **S3 - Lorentzian -**
  $V_{de} = 2.0 \times \theta$
  $(\theta = [(2\kappa-3)/2\kappa]^{1/2} (2T/m)^{1/2})$
  Nz=625, Nve=2777, Nvi=215
- $M_i = 25\, m_e$
- $T_i = T_e = 1$ eV
- $n_i = n_e = 7 \times 10^6 /m^3$
- Equal velocity grid resolution
- $\kappa = 2$

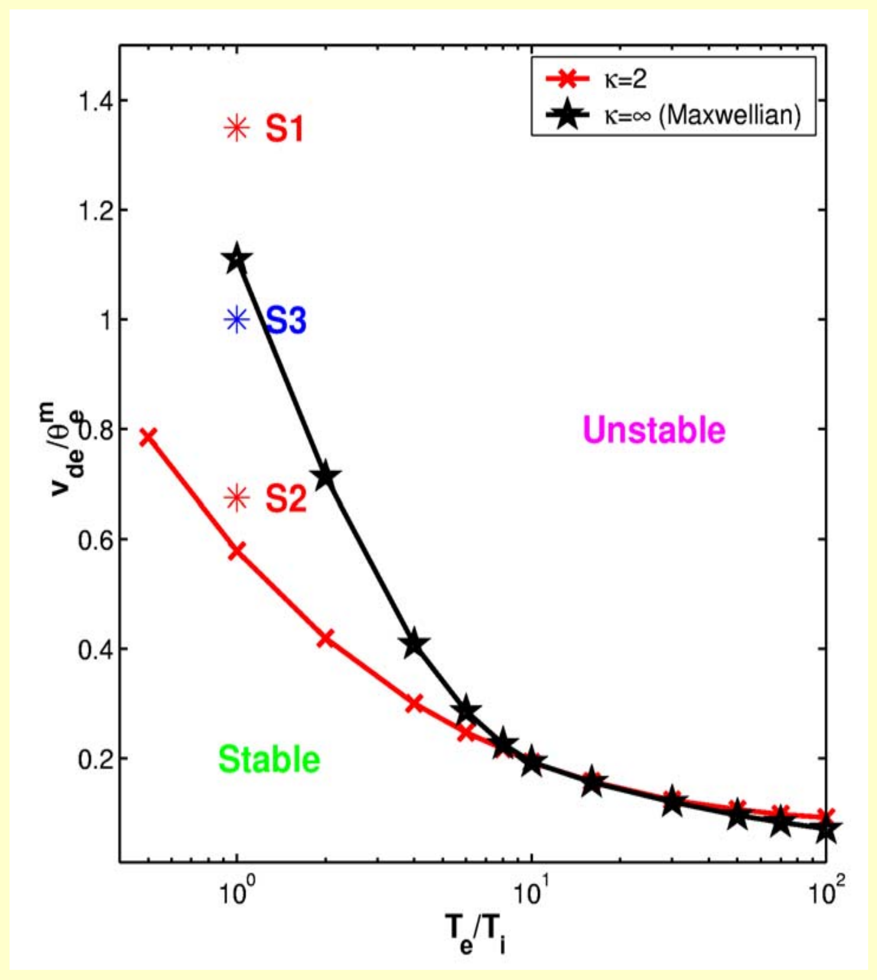

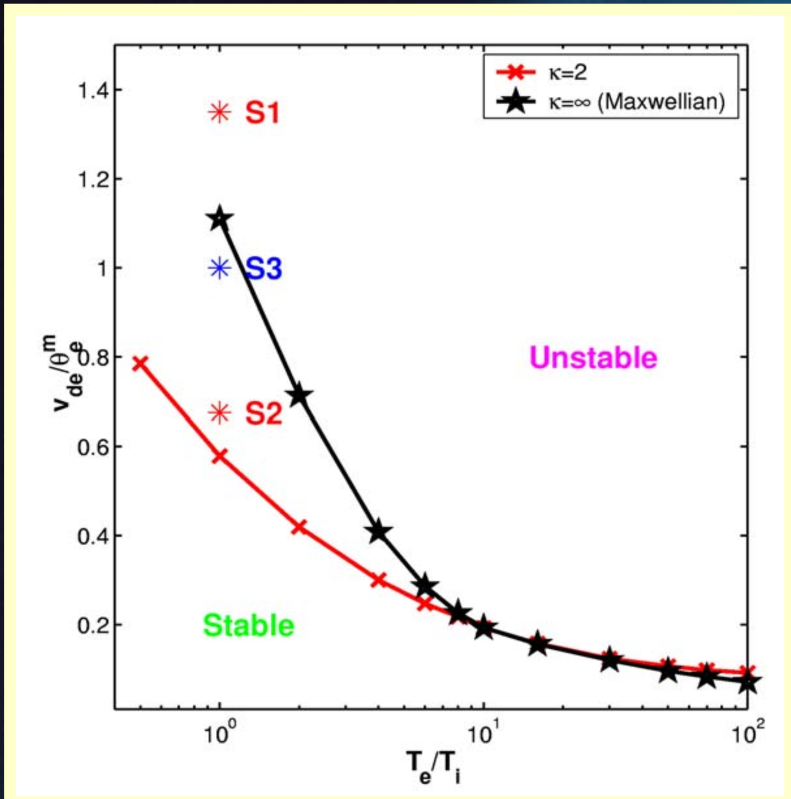

Lorentzian S3

Resistivity at saturation ~ 2000 Ohm m

Quasi-linear saturation

Plateau Formation

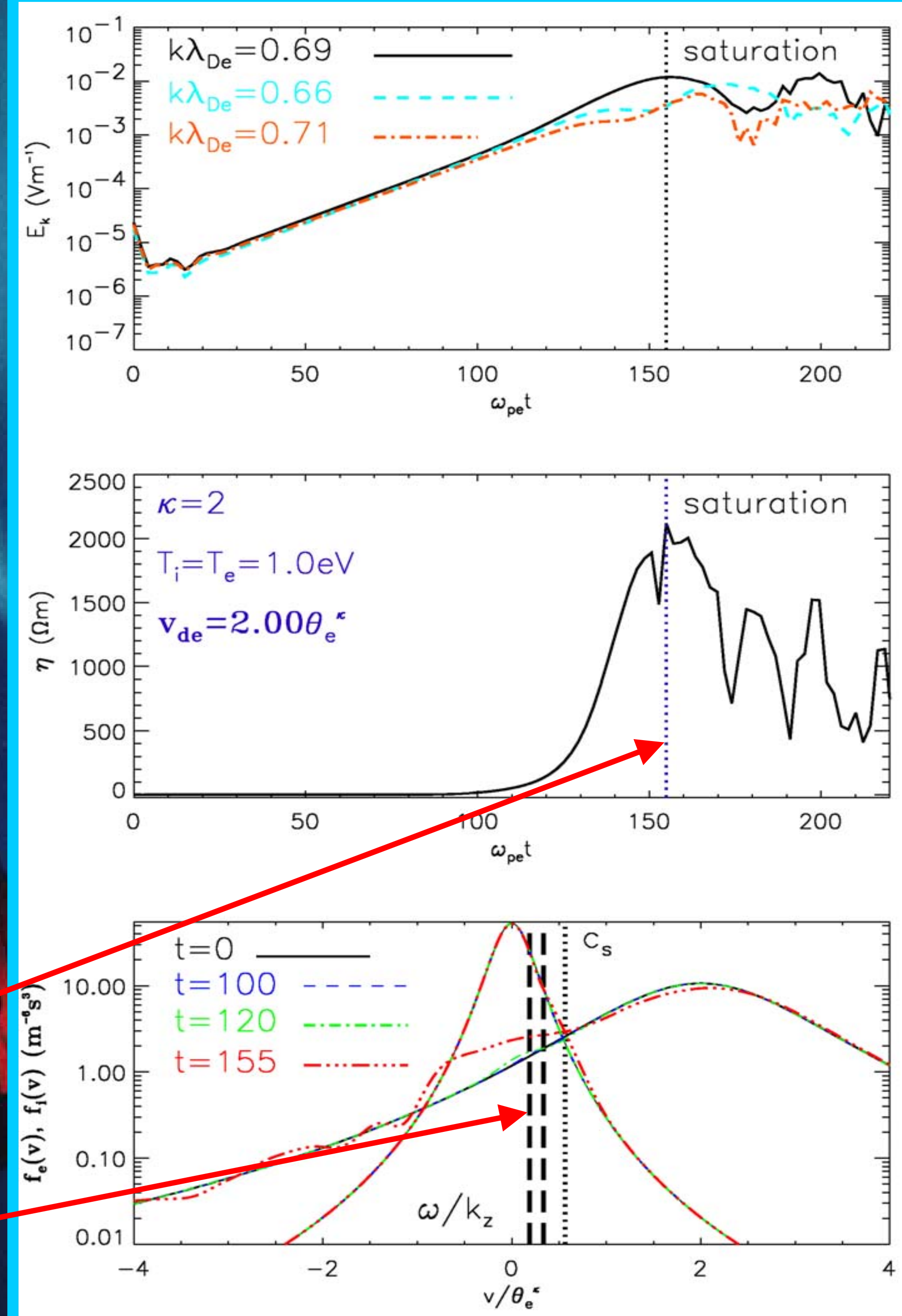

Conclusions on The Ion-Acoustic Resistivity

1. Calculated ion-acoustic anomalous resistivity for space plasmas conditions, for low $T_e/T_i \leq 4$, Lorentzian DF.
2. A Lorentzian DF enables significant anomalous resistivity for conditions where none would result for a Maxwellian DF.
3. At wave saturation, the anomalous resistivity for a Lorentzian DF can be an order of magnitude higher than that for a Maxwellian DF, even when the drift velocity and current density for the Maxwellian case are larger.
4. The anomalous resistivity resulting from ion acoustic waves in a Lorentzian plasma is strongly dependent on the electron drift velocity, and can vary by a factor of $\approx$ 100 for a 1.5 increase in the electron drift velocity.
5. Anomalous resistivity seen in 1-D simulation
6. Resistivity I) Corona = 0.1 Ω m, II) Magnetosphere = 0.001 Ω m

Resistivity in Collisionless Plasmas

- Resistivity from Wave-Particle interactions is important in Collisionless plasmas
- We have studied resistivity from Current Driven Ion-Acoustic Waves (CDIAW)
  - Used Vlasov Simulations
  - Realistic plasma conditions i.e. $T_e \sim T_i$, Maxwellian and Lorentzian distribution function
  - Found Substantial resistivity at quasi-linear saturation
- What happens after quasi-linear saturation
- Study resistivity from the nonlinear evolution of CDIAW
- We investigate the non-linear evolution of the ion-acoustic instability and its resulting anomalous resistivity by examining the properties of a statistical ensemble of Vlasov simulations.

Ion-Acoustic Resistivity Post-Quasilinear Saturation

- Resistivity at saturation of fastest growing mode
- Resistivity after saturation also important
  - Behaviour of resistivity highly variable
- Ensemble of simulation runs – probability distribution of resistivity values, study its evolution in time
  - Evolution of each individual simulation in the nonlinear regime is very sensitive to initial noise field
  - Require Statistical Approach
- 104 ensemble run on High Performance Computing (HPCx) Edinburgh (1280 IBM POWER4 processors)

Superposition of the time evolution of ion-acoustic anomalous resistivity of 3 Vlasov Simulations

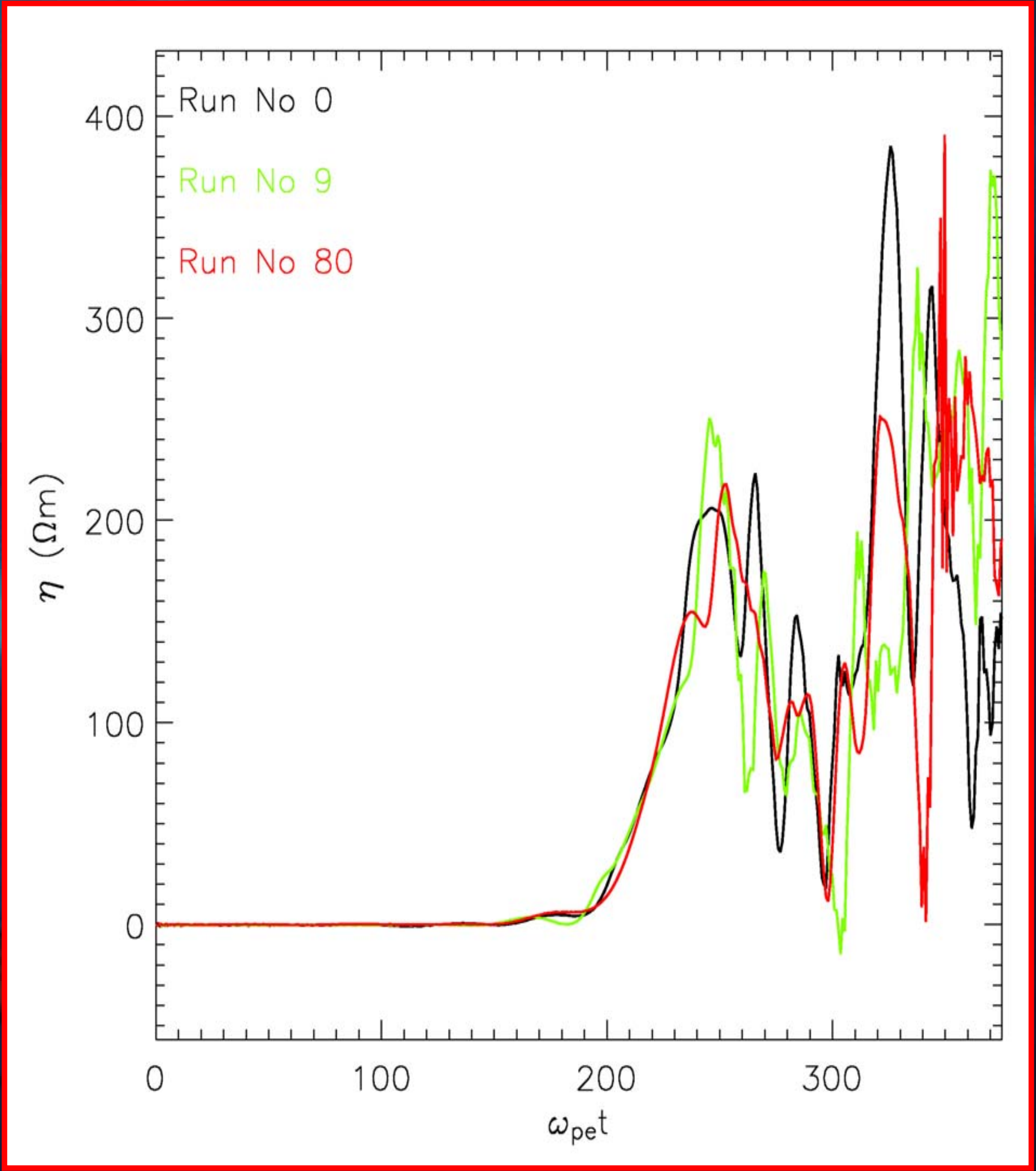

Superposition of the time evolution of ion-acoustic anomalous resistivity of 104 Vlasov Simulations

Superposition of the time evolution of ion-acoustic wave energy of 104 Vlasov Simulations

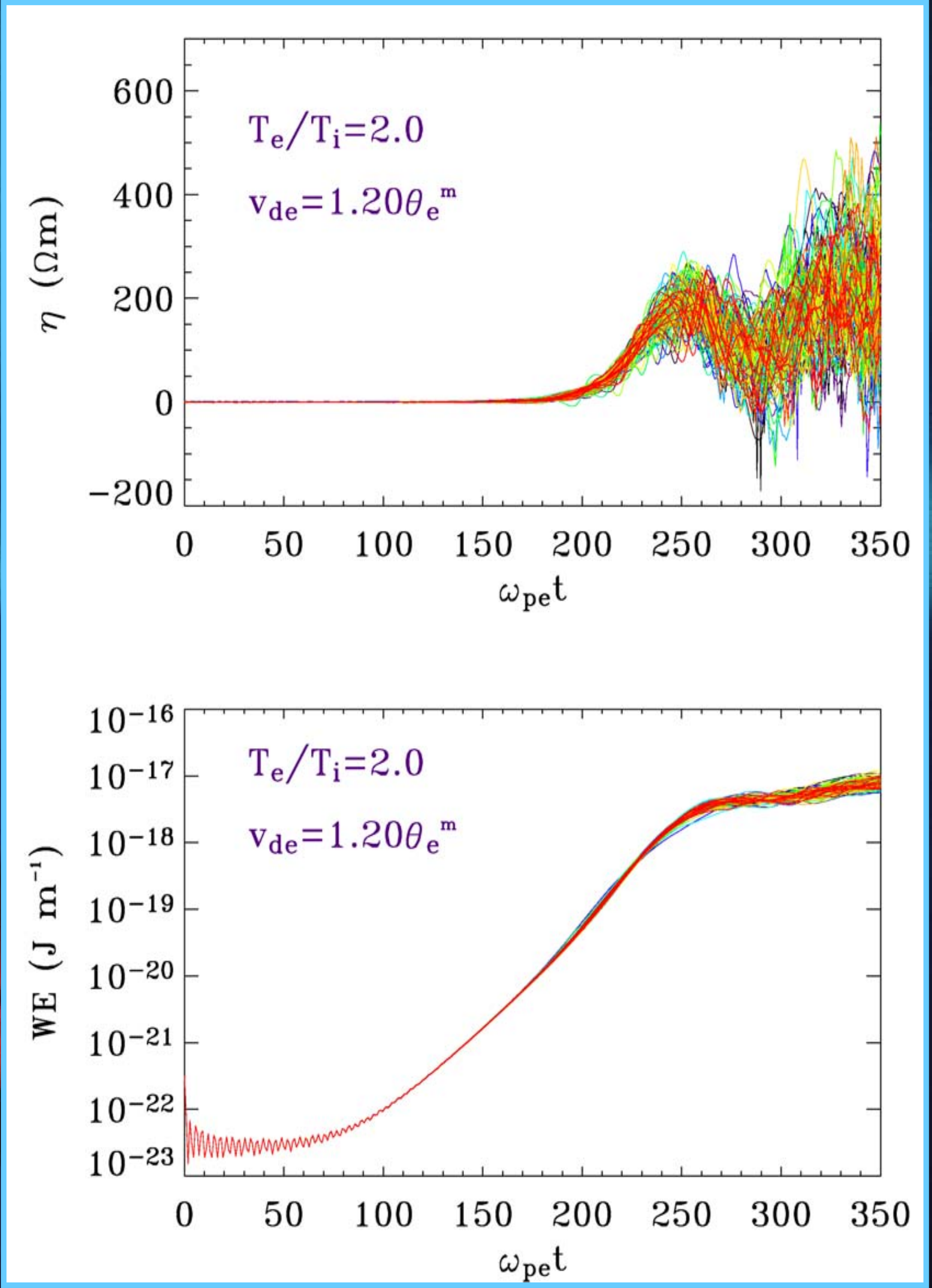

Mean of the ion-acoustic anomalous resistivity ± 3 standard deviations

Mean of the ion-acoustic wave energy ± 3 standard deviation

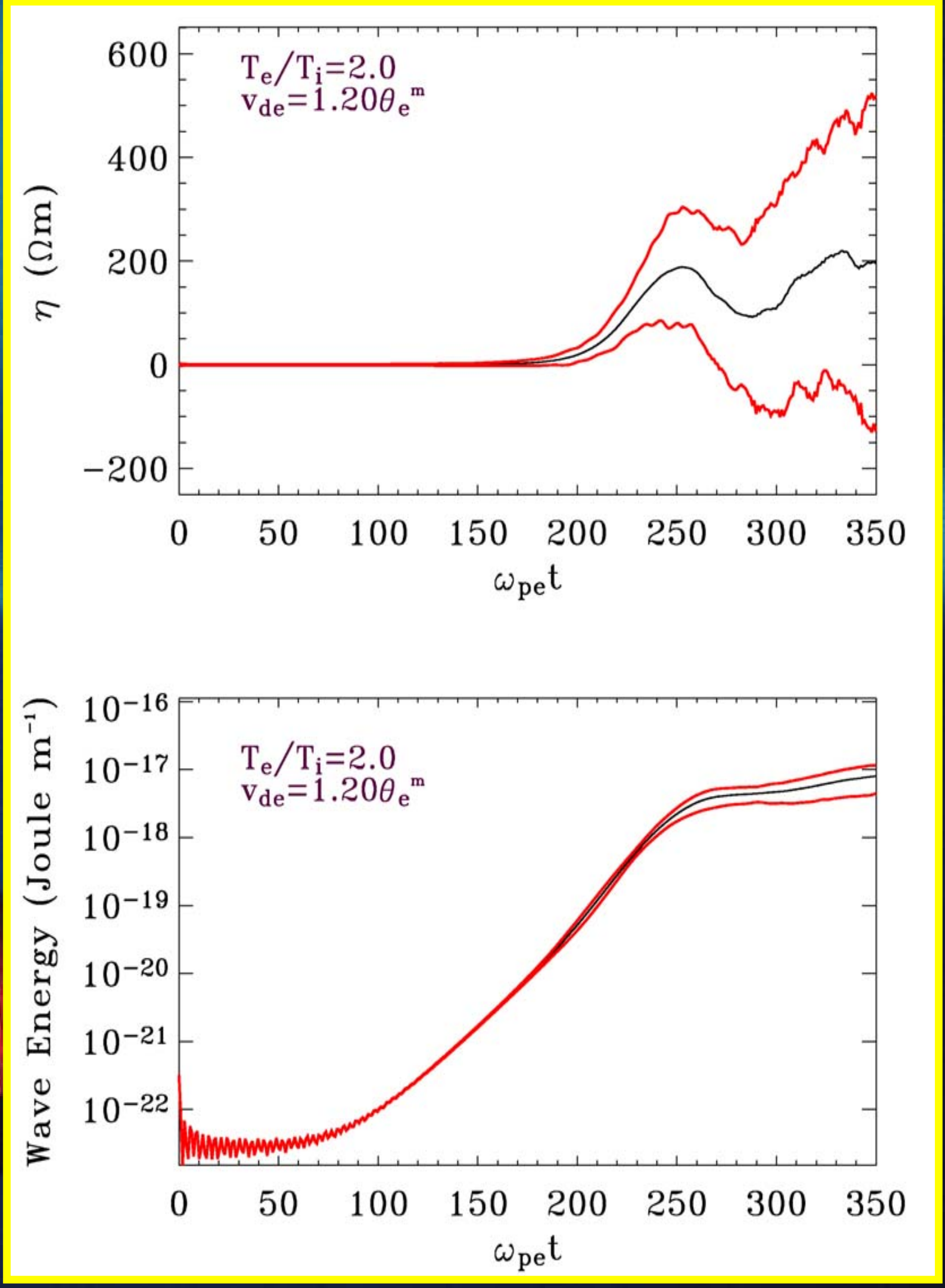

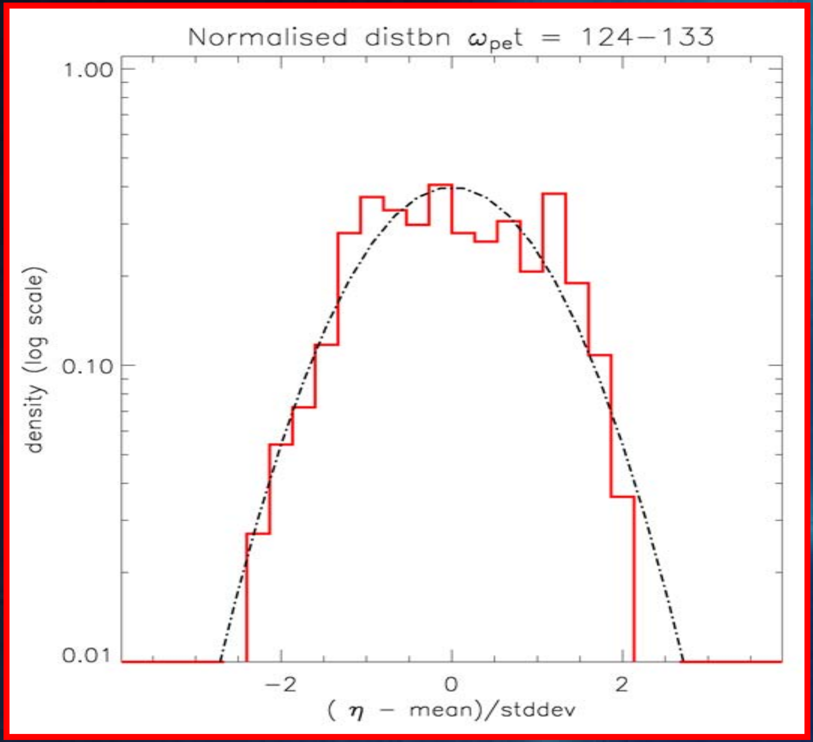

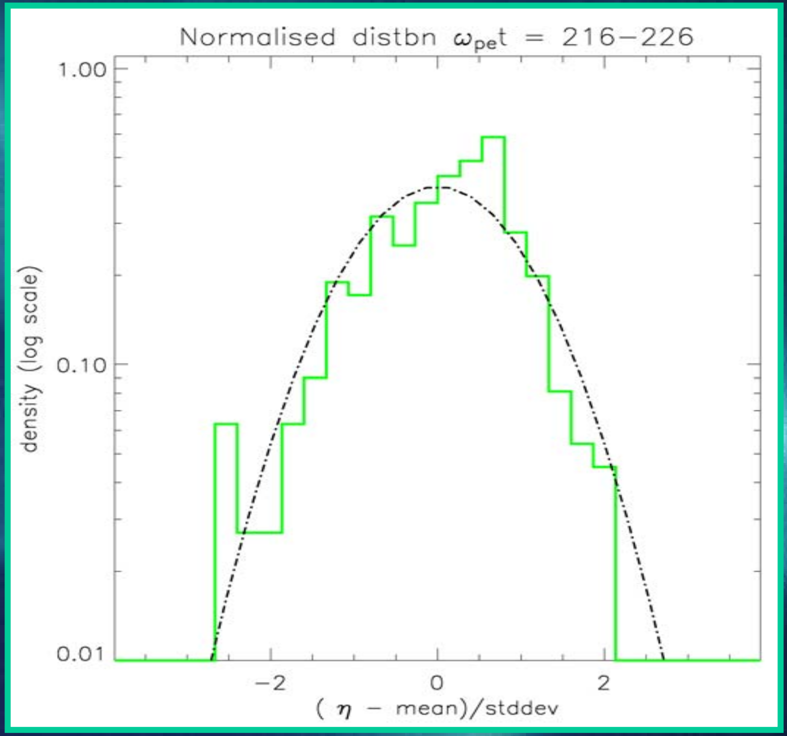

PD of resistivity values in the Linear phase

PD of resistivity values at Quasilinear phase

Approximately Gaussian?

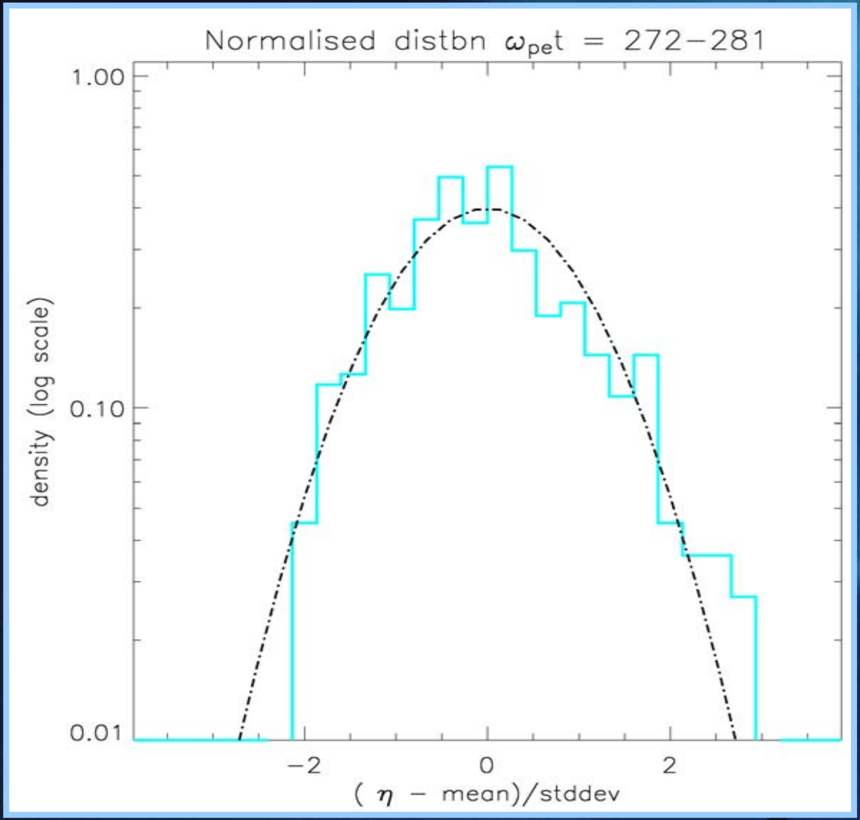

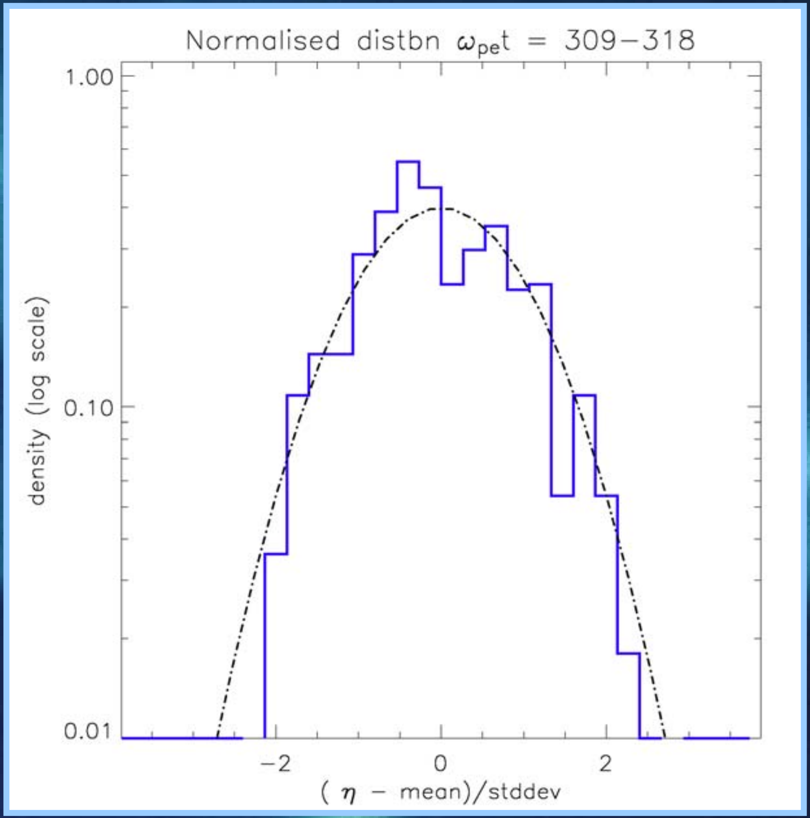

PD of resistivity values after Quasilinear phase

PD of resistivity values in Nonlinear phase

Distribution in Nonlinear regime Gaussian?

Histogram of Anomalous resistivity values

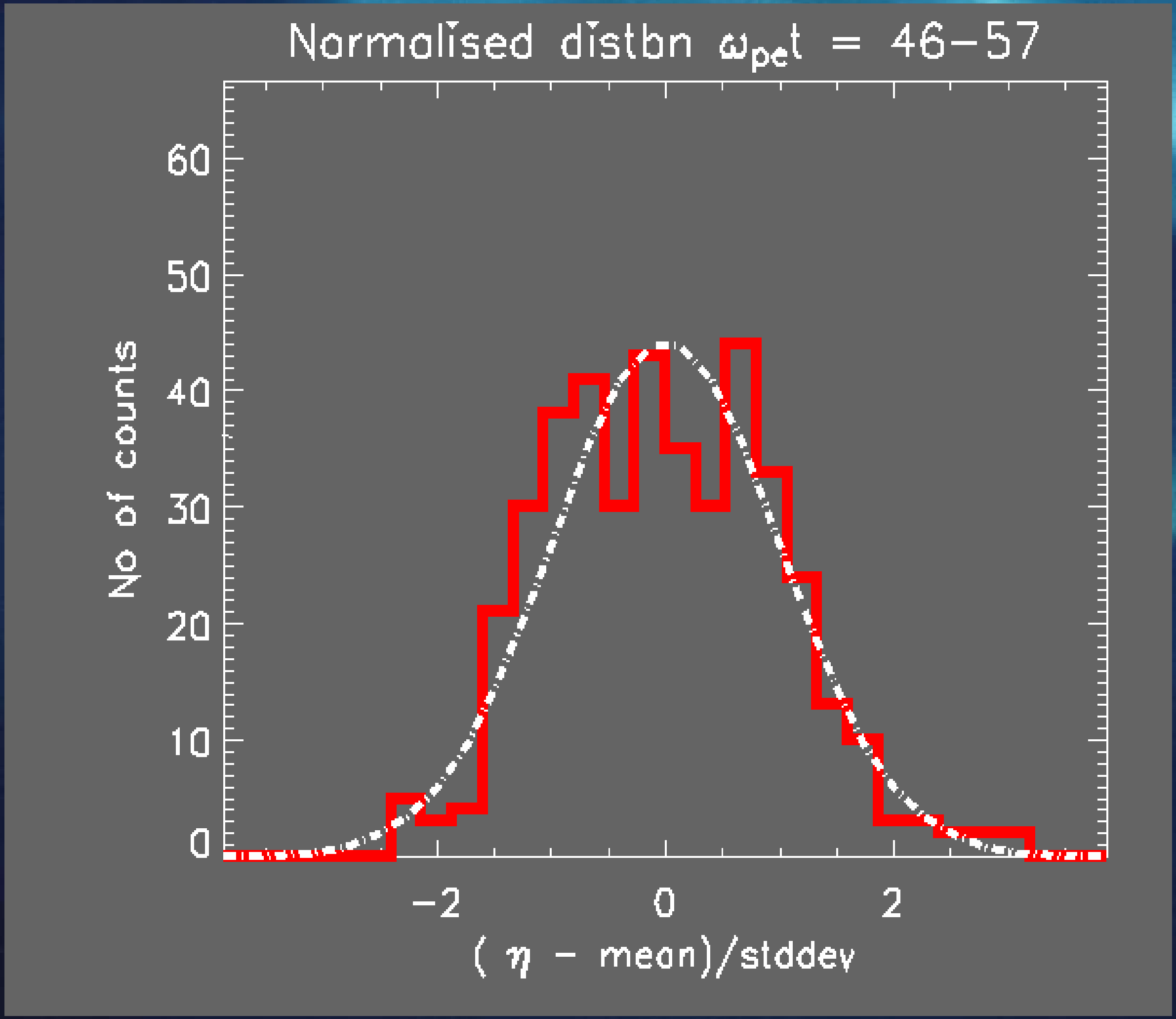

Skewness and kurtosis of probability distribution of resistivity values

skewness = 0
kurtosis = 3
for a Gaussian

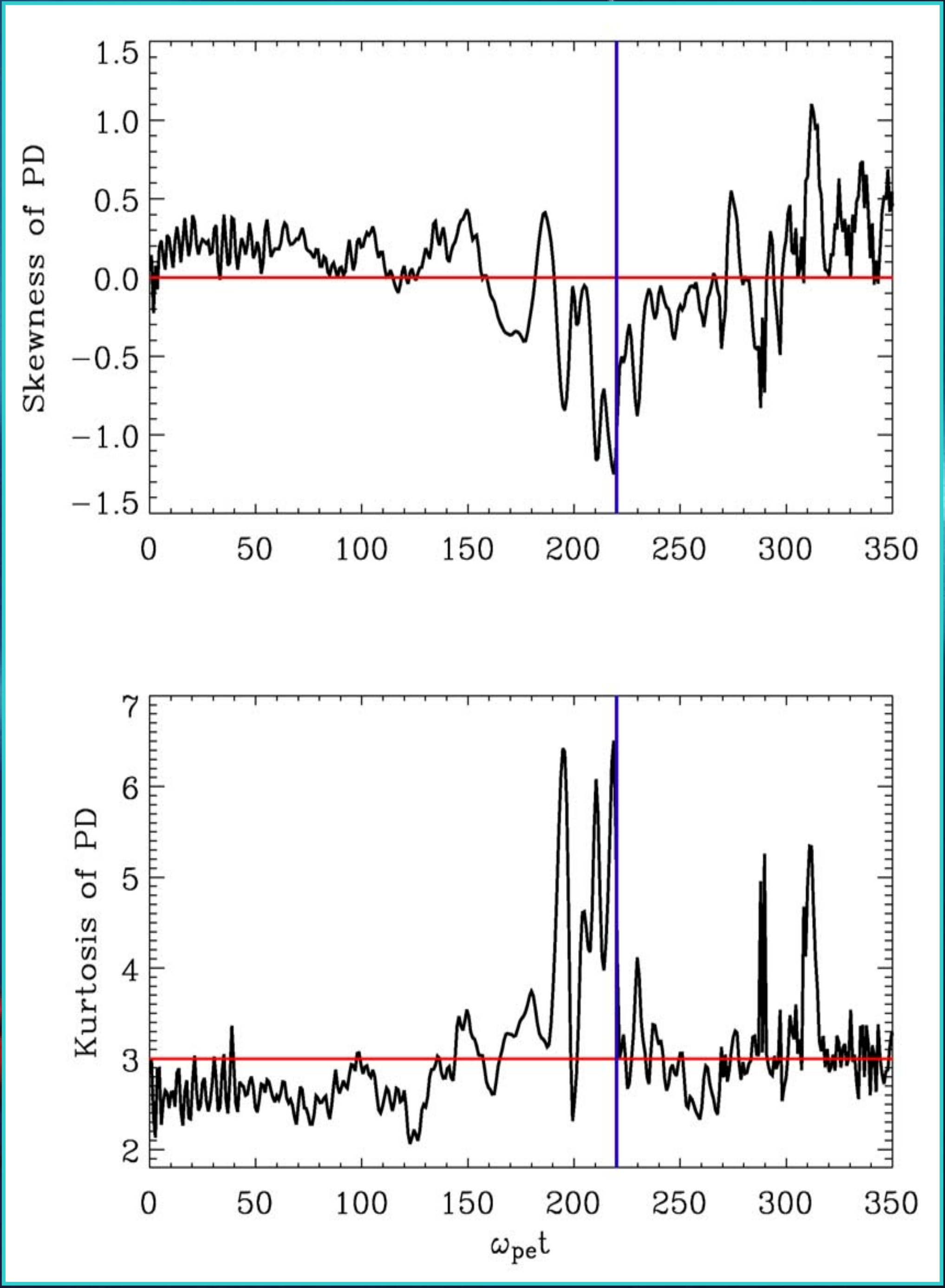

Discussion

- Ensemble of 104 Vlasov Simulations of the current driven ion-acoustic instability with identical initial conditions except for the initial phase of noise field
- Variations of the resistivity value observed in the quasilinear and nonlinear phase
- The probability distribution of resistivity values Gaussian in Linear, Quasilinear, Non-linear phase
- A well-bounded uncertainty can be placed on any single estimate of resistivity, e.g., at quasi-linear saturation
- Estimation at quasi-linear saturation provides underestimation of Resistivity
- May affect likehood of magnetic reconnection and current sheet structure

References

1. Petkaki P., Watt C.E.J., Horne R., Freeman M., 108, A12, 1442, 10.1029/2003JA010092, JGR, 2003
2. Watt C.E.J., Horne R. Freeman M., Geoph. Res. Lett., 29, 10.1029/2001GL013451, 2002
3. Petkaki P., Freeman M., Kirk T., Watt C.E.J., Horne R., submitted to JGR

CLUSTER observations of waves in and around a possible reconnection diffusion region in the Earth's magnetotail current sheet.

Panagiota Petkaki[1], Andrew Walsh[1], Mervyn Freeman[1],
Andy Buckley[2], Chris Owen[3],
Elizabeth Lucek[4], Richard Horne[1],
Nicole Cornilleau – Wehrlin[5]

[1] British Antarctic Survey, [2] The University of Sussex, [3] MSSL, [4] Imperial College, [5] CETP/UVSQ

Cluster Tail event
11-Oct-2001 3:25-3:45

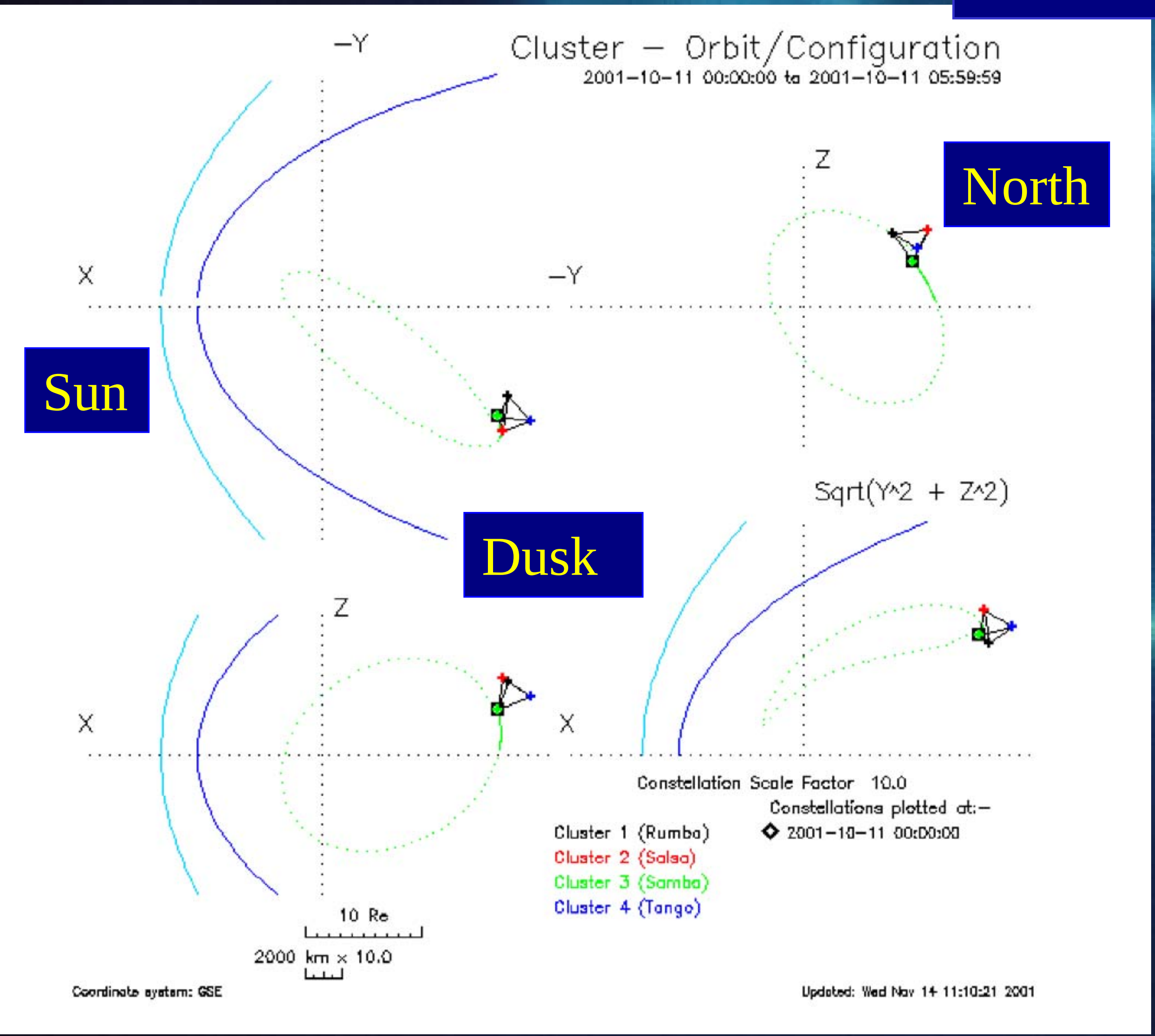

1500 Km separation in Z

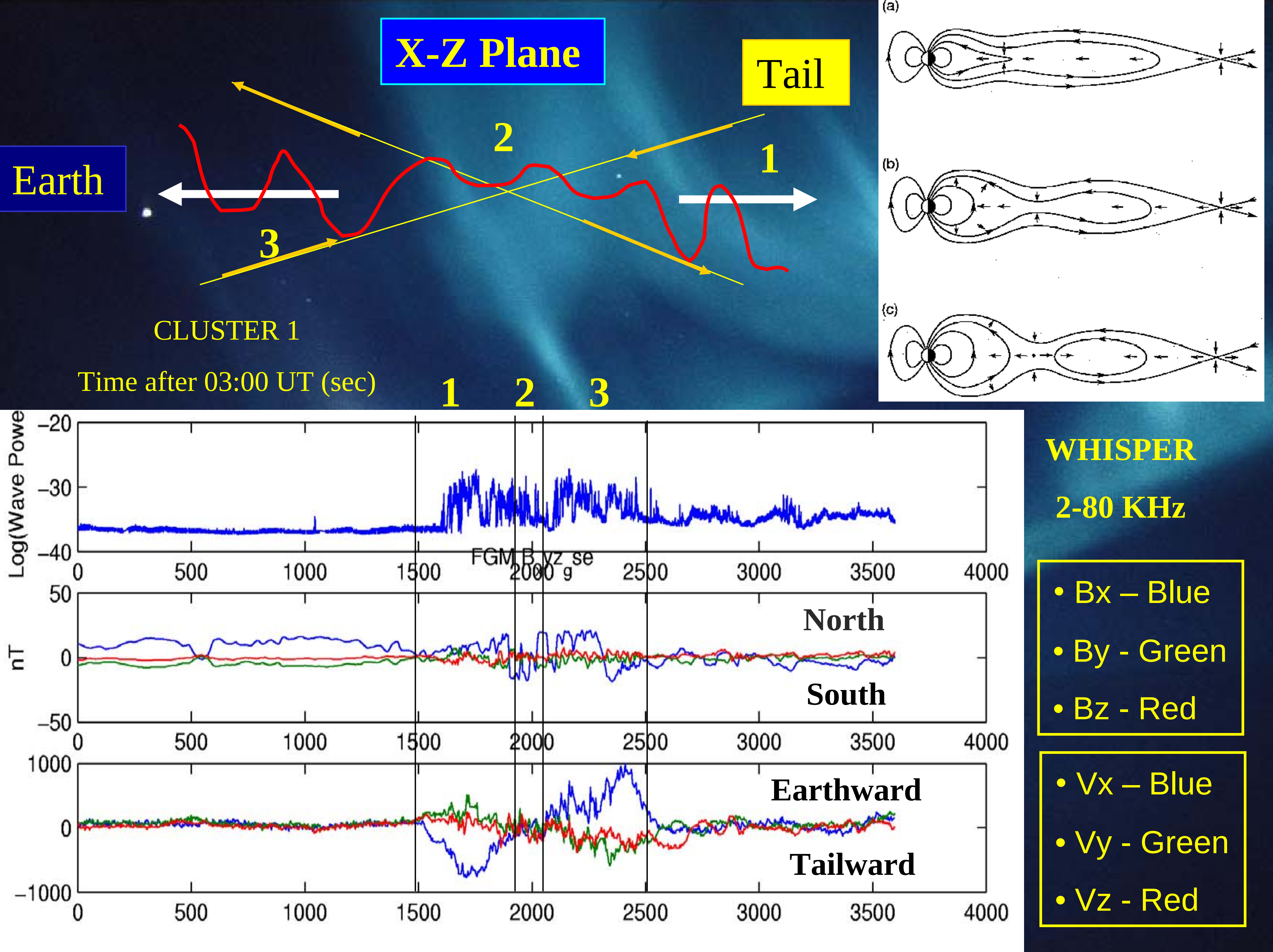

X-Z Plane
Tail
Earth
1
2
3
(a)
(b)
(c)
CLUSTER 1
Time after 03:00 UT (sec)
1 2 3
Log(Wave Powe
nT
North
South
Earthward
Tailward
WHISPER
2-80 KHz
• Bx – Blue
• By - Green
• Bz - Red
• Vx – Blue
• Vy - Green
• Vz - Red

1. Cluster move from northern lobe (+ Bx, blue) to southern lobe (- Bx, blue) over whole interval, making several current sheet crossings.
2. Flows reverse from tailward (- Vx, blue) to earthward (+ Vx, blue), suggesting reconnection site moves over spacecraft.
3. Strong wave activity is seen. Want to know how this is related to reconnecting current sheet structure.

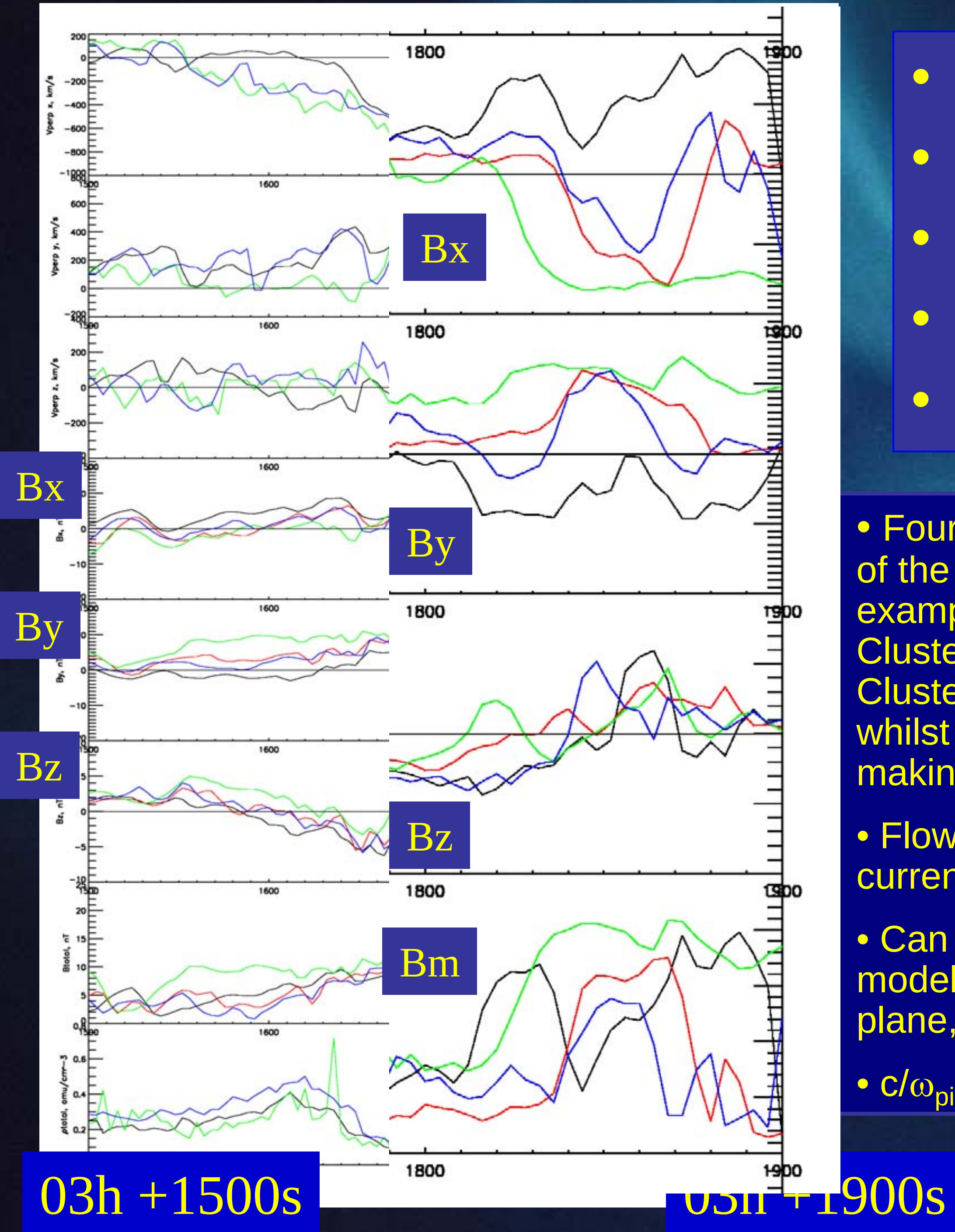

- 11/10/2001 – 0300
- Vperp, x,y,z (km/s)
- Bx,By,Bz (nT)
- Btotal (nT)
- ρ total (amu/cm^{-3})

- Four spacecraft encounter different parts of the current sheet simultaneously. For example between t =1850 and t = 1900 Cluster 1 (black) is in the northern lobe and Cluster 3 (green) is in the southern lobe whilst Cluster 2 (red) and 4 (blue) are making several current sheet crossings.

- Flow is tailward (- Vx) on both sides of the current sheet.

- Can we use the four spacecraft to create a model of the current sheet profile in x-z plane, or even a model of its 3-D structure?

- c/ω_{pi} = 500 Km, 1500 Km separation in Z

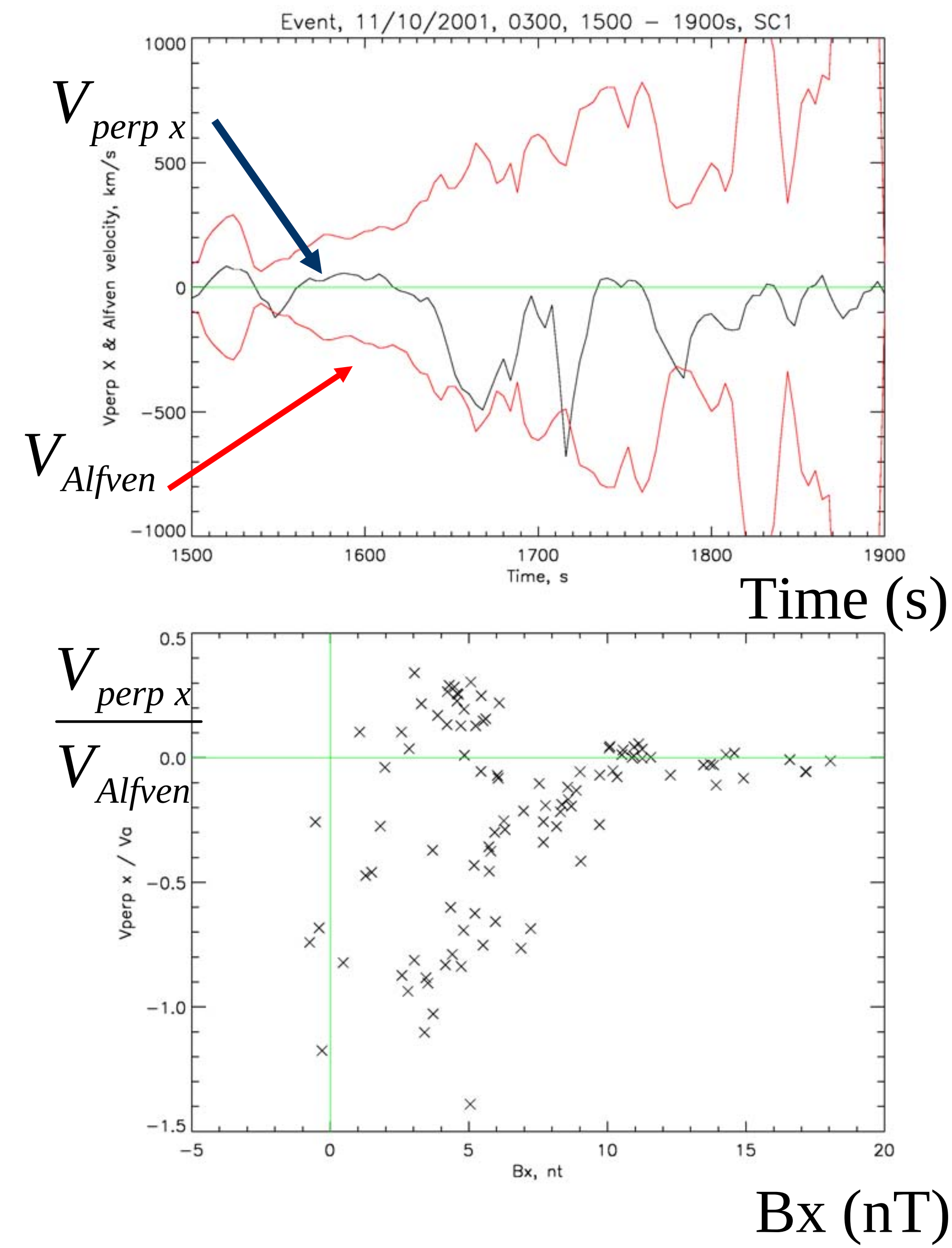

- **SC1 – Calculated Alfvén speed**
- **Earthward component (x) of the ExB flow**
- **Local Alfven speed (magnetic field and density measurements).**
- **The flow is sometimes Alfvénic.**
- **These times correspond to when the spacecraft is in the current sheet (low Alfvén speed).**
- **Provides further support for reconnection structure.**

Cluster 1 : STAFF overplotted |B|

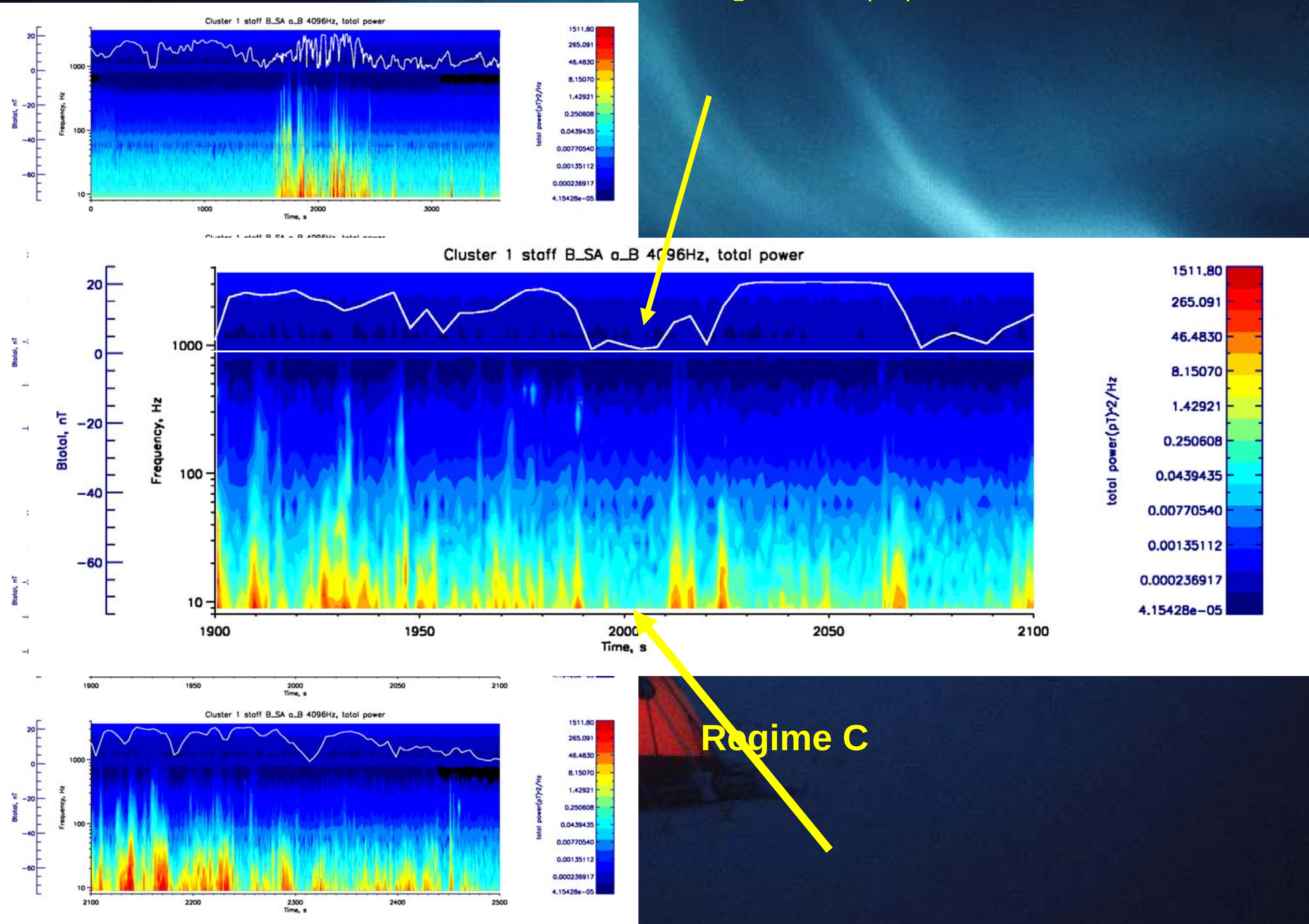

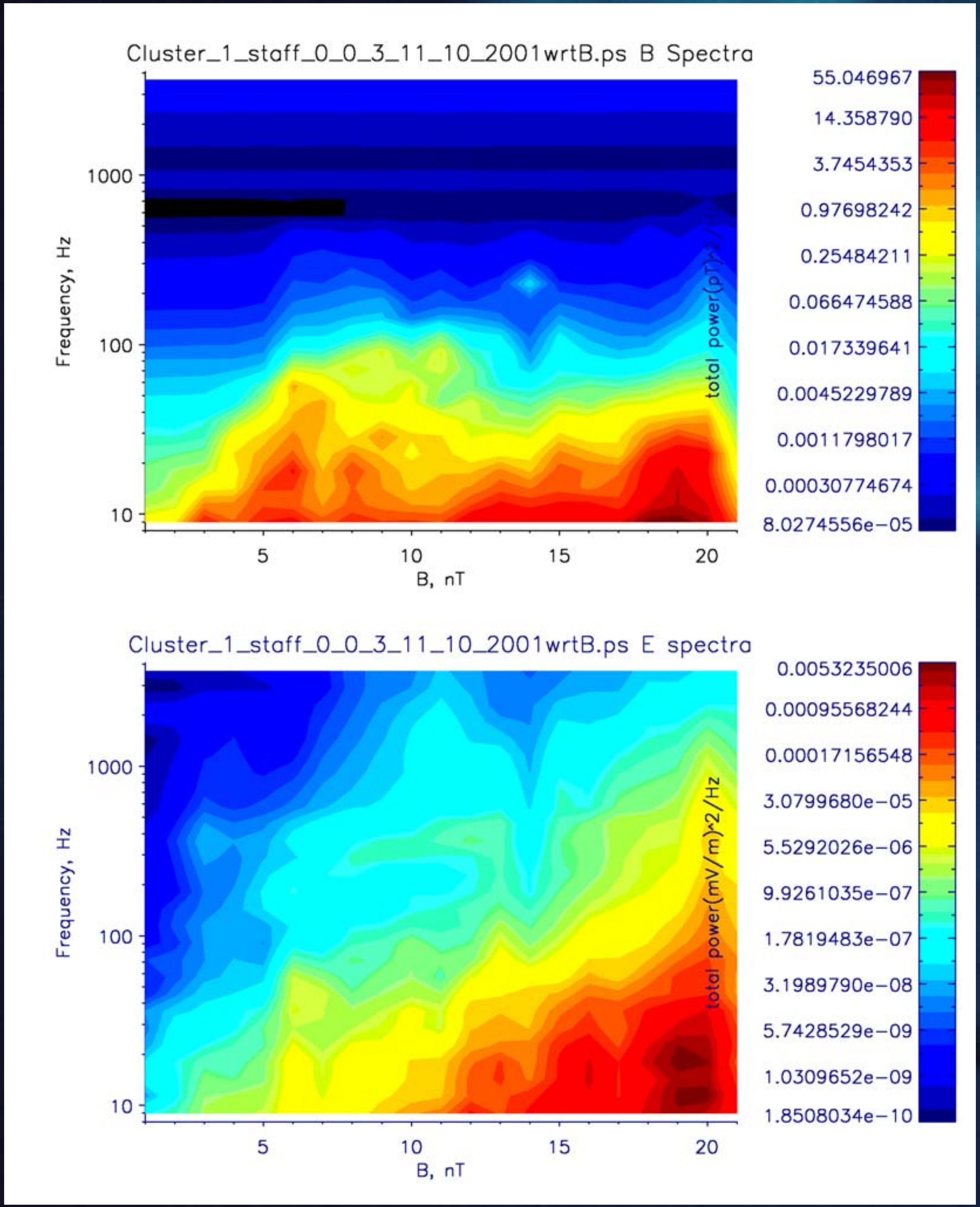

- **Cluster Spacecraft 1**
- **Magnetic and Electric Spectra with respect to magnitude of the magnetic field**
- **Regime A+B+C (1500-2500)**
- **F_{ce} (Hz) = 28 B (nT)**

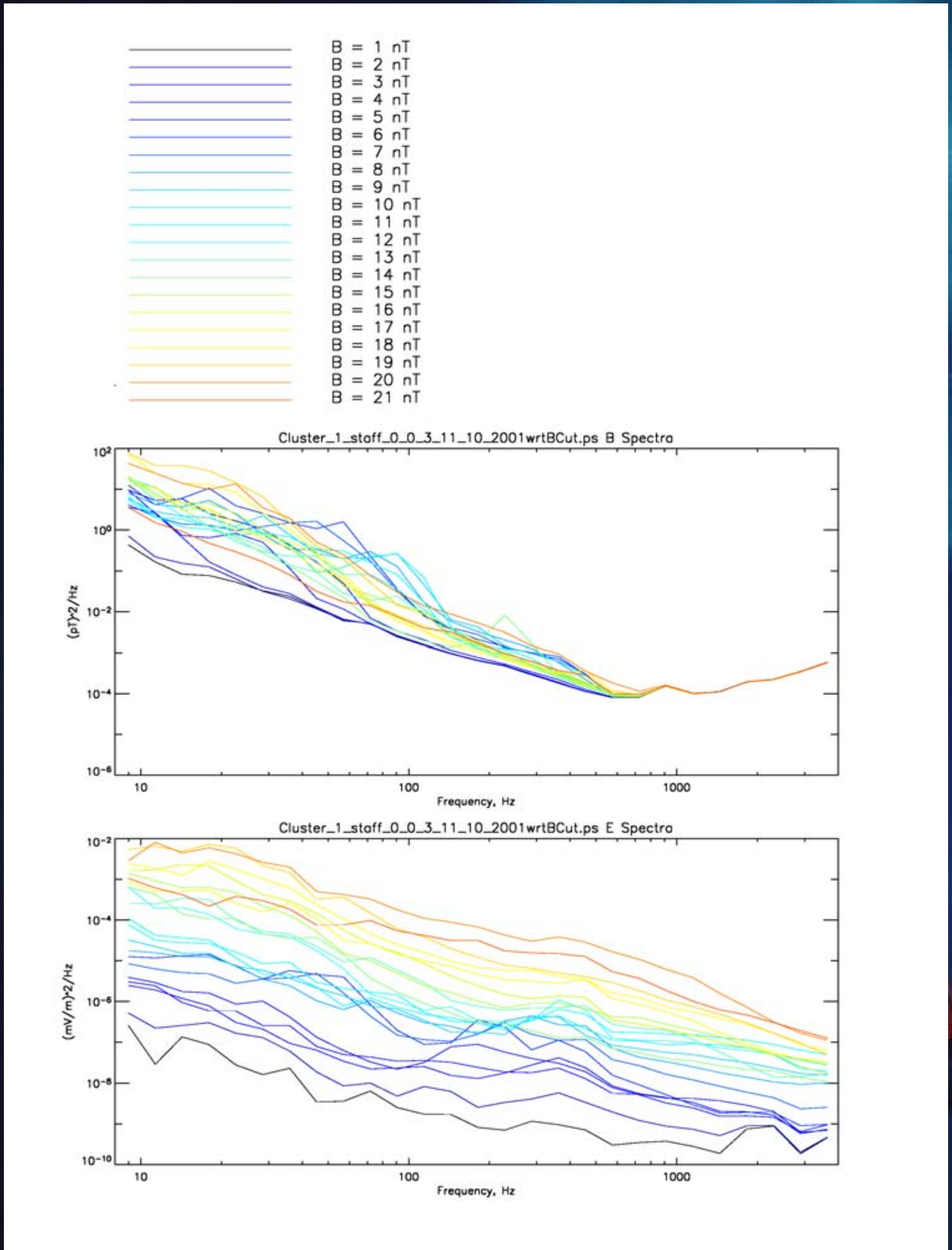

1. Re-ordering spectra by the background magnetic field strength (i.e., finding average spectrum for all occasions when B = 1, 2, 3 nT, etc.) confirms that wave power is reduced in center of current sheet where B is small and maximizes in the lobes.
2. E-field spectrum is unstructured - turbulent cascade.
3. B-field spectrum shows some evidence of linear wave mode at few tens of Hz

Wave Power in terms of |B|

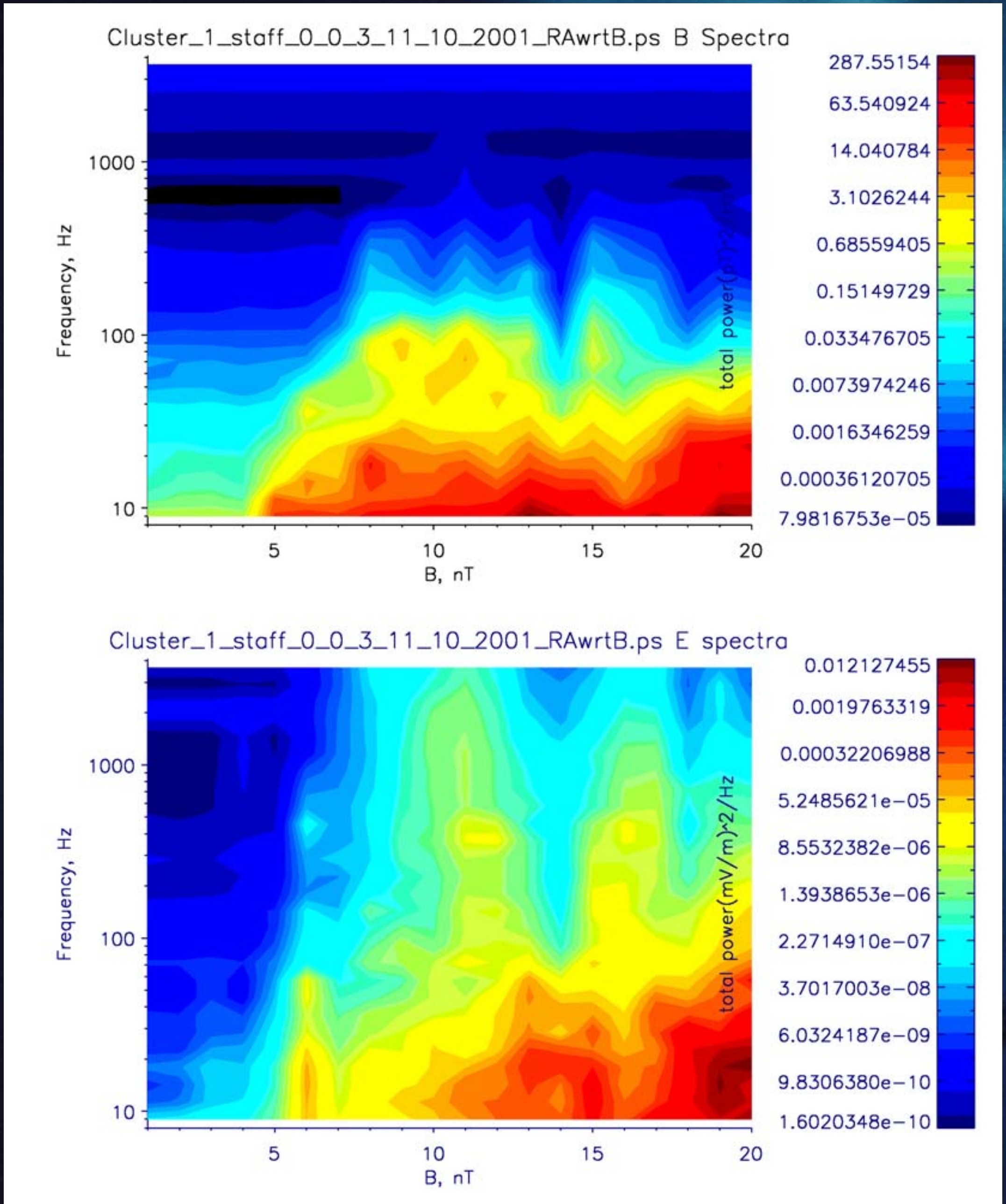

- Spacecraft 1 : Spectra with respect to the magnetic field
- Regime A (1500-1900)
- Regime B (1900-2100)
- Regime C (2100-2500)
- Wave power is ordered by the magnitude of the magnetic field.
- When magnetic field strength goes to zero then wave power decreases (similarly for E-field spectrum).
- Suggests that there are no waves in the center of the current sheet?

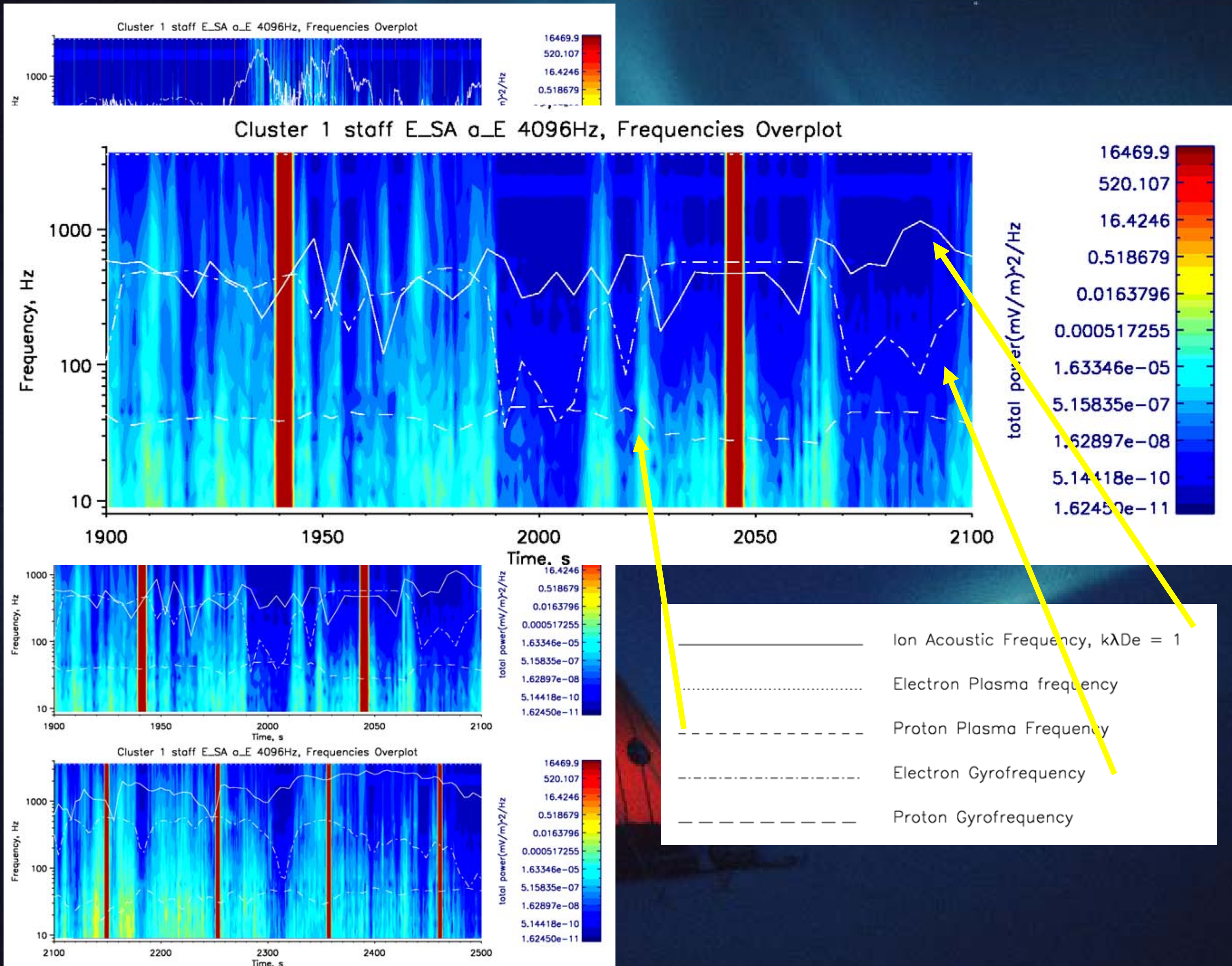
Cluster 1 staff E_SA a_E 4096Hz, Frequencies Overplot
Frequency, Hz
1000
100
10
1900
1950
2000
2050
2100
Time, s
total power(mV/m)^2/Hz
16469.9
520.107
16.4246
0.518679
0.0163796
0.000517255
1.63346e-05
5.15835e-07
1.62897e-08
5.14418e-10
1.62450e-11
Ion Acoustic Frequency, kλDe = 1
Electron Plasma frequency
Proton Plasma Frequency
Electron Gyrofrequency
Proton Gyrofrequency
Cluster 1 staff E_SA a_E 4096Hz, Frequencies Overplot
2100
2200
2300
2400
2500
Time, s

Electric field Spectra

- Electric field Wave spectrum from 8Hz to 4 kHz shows broadband activity.
- Little evidence of linear wave modes (i.e., enhancement of wave power at frequencies predicted by linear theory and shown on the plot).
- Possibly a nonlinear cascade from lower hybrid waves at frequency < 10 Hz?

Summary

1. Analysis of electric and magnetic waves from 8 to 4000 Hz measured by STAFF instruments on the Cluster spacecraft during several current sheet crossings on 11/10/2001.
2. Plasma flows of order of the local Alfvén speed reversed from tailward to earthward, suggesting a possible reconnection site moved over spacecraft.
3. Strong broadband electric and magnetic wave activity during the interval with little evidence of discrete linear wave modes.
4. Ordered the observed wave spectrum by the position within the current using the magnitude of the magnetic field.
5. Found that the electric and magnetic wave power decreased considerably at all frequencies when the magnetic field strength approached zero.
6. Electrostatic and electromagnetic waves might be efficiently suppressed within the current sheet.
7. Reconnection from wave-particle interactions?

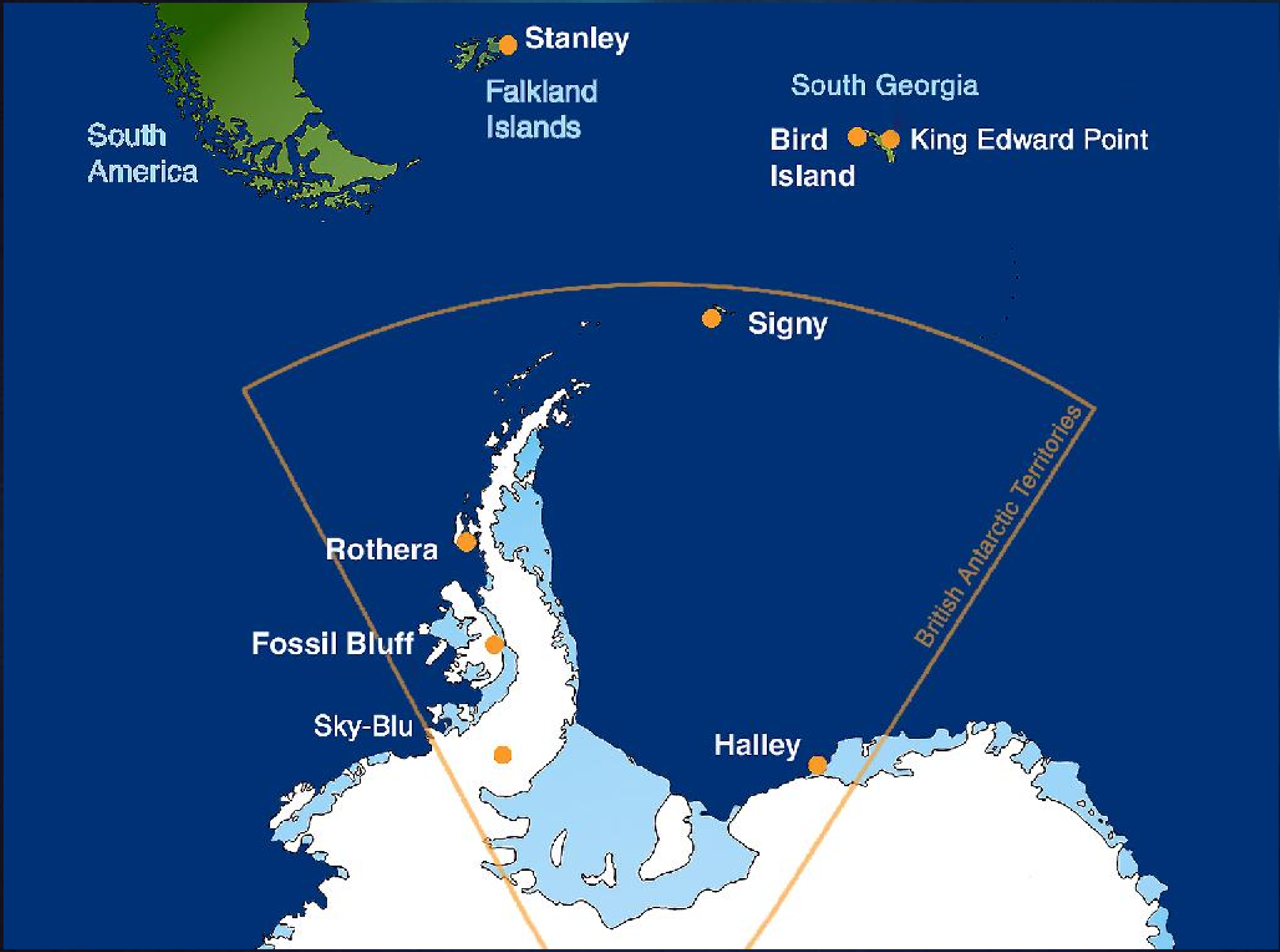
Stanley
Falkland Islands
South Georgia
South America
Bird Island
King Edward Point
Signy
British Antarctic Territories
Rothera
Fossil Bluff
Sky-Blu
Halley

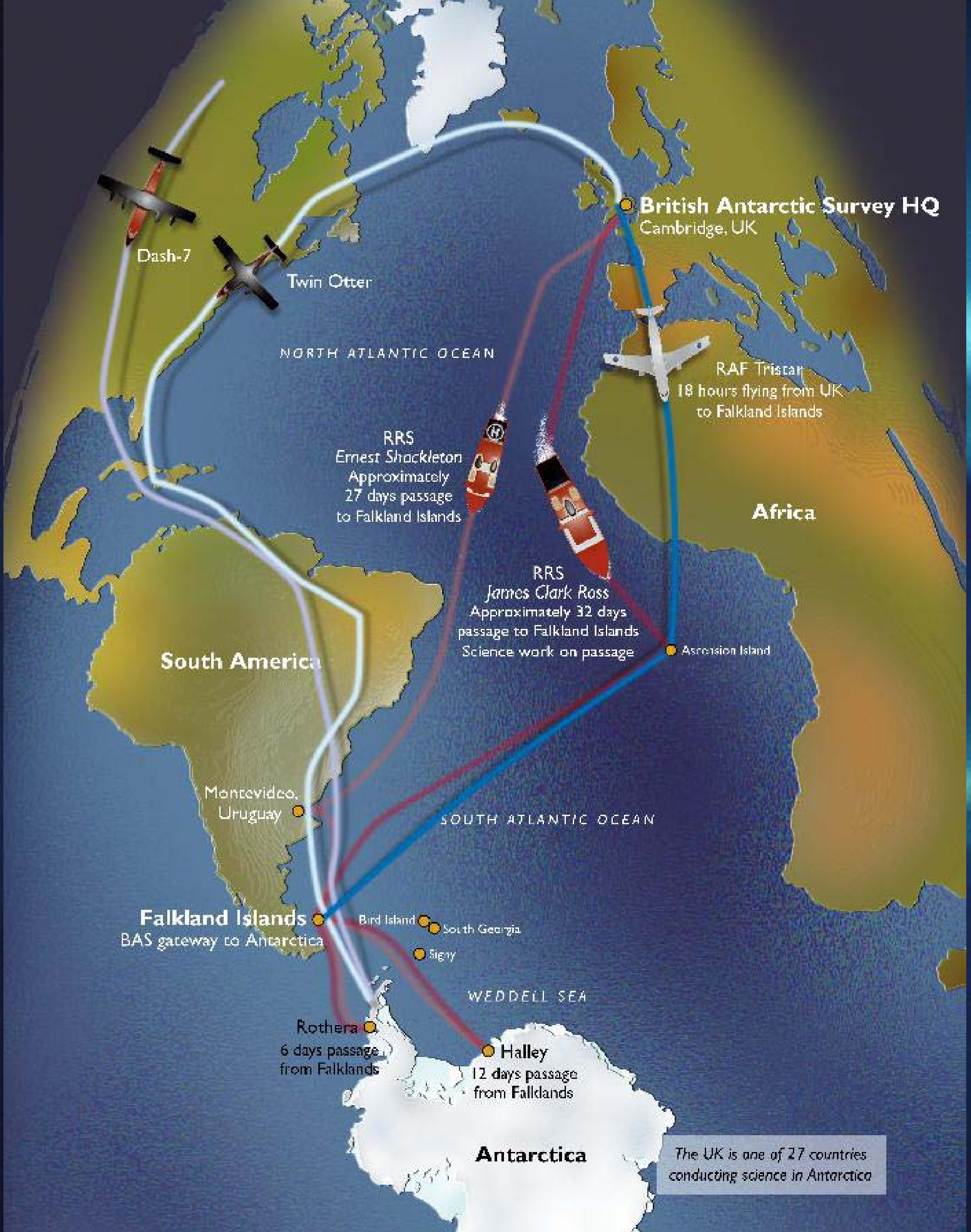
British Antarctic Survey HQ
Cambridge, UK
Dash-7
Twin Otter
NORTH ATLANTIC OCEAN
RAF Tristar
18 hours flying from UK
to Falkland Islands
RRS
Ernest Shackleton
Approximately
27 days passage
to Falkland Islands
Africa
RRS
James Clark Ross
Approximately 32 days
passage to Falkland Islands
Science work on passage
Ascension Island
South America
Montevideo,
Uruguay
SOUTH ATLANTIC OCEAN
Falkland Islands
BAS gateway to Antarctica
Bird Island
South Georgia
Signy
WEDDELL SEA
Rothera
6 days passage
from Falklands
Halley
12 days passage
from Falklands
Antarctica
The UK is one of 27 countries
conducting science in Antarctica

Rothera Research Station, Adelaide Island (67° 34' S, 68° 08' W), Antarctica

Halley Research Station, Coats Land (75° 35' S, 26° 34' W)

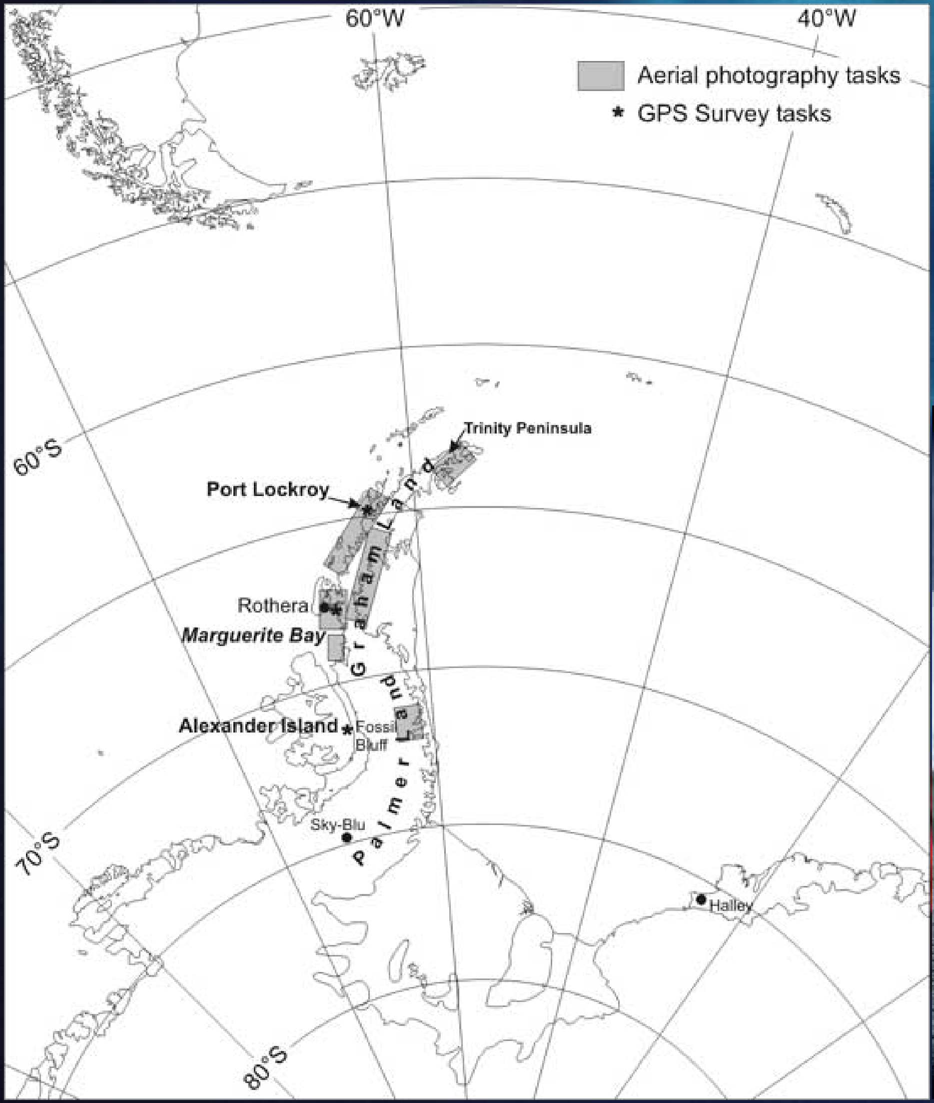

Natural Complexity

- **COMPLEXITY will apply new mathematical methods to data sets drawn from across the *Global Science in the Antarctic Context* programme to reveal previously hidden underlying patterns and laws, and to develop new mathematical models to explain them. This is known as the field of complexity science. Combined with results from other BAS scientific programmes this work will help assess the likelihood of extreme environmental changes.**

Objectives

- **Identify, measure and explain aspects of complexity in four main components of the Earth system – the atmosphere, biosphere, cryosphere, and magnetosphere**
- **Use ideas and methods from complexity science to offer new insights into environmental problems under investigation in selected BAS science programmes**

Sun Earth Connections Programme (SEC)

- SEC will describe and quantify the key mechanisms by which variations in the solar wind and solar high-energy radiation affect the Earth's atmosphere, to determine whether or not these have a significant effect on the Earth's climate system. It will look at the atmosphere and geospace as a unified whole, opening the way to the development of more realistic numerical models of the climate system

Objectives

- Quantify the key mechanisms of indirect links between the Sun and the Earth's atmosphere
- Determine how the effect of solar variability may be amplified through those links and the significance for climate
- Determine the evolution of atmospheric change over time due to indirect influences, on different timescales and at different epochs

Greenhouse to ice-house: Evolution of the Antarctic Cryosphere And Palaeoenvironment (GEACEP)

- GEACEP will investigate the relationship between the evolution of Antarctic ice and the changing global environment over the last ~30 million years (My). We will do so through collecting and combining geological data and developing computer models of the Earth as an integrated system. The aim is to clarify the forcing and feedback mechanisms responsible for the formation of large-scale Antarctic ice cover, and to examine the stability of the permanent Antarctic ice sheet over its ~20My history. We will use the resulting insights to check and improve the performance of computer models – known as General Circulation Models – used for the prediction of climate change.

Objectives

- Examine the nature of past warm climates over the last 30My
- Clarify the forcing and feedback mechanisms associated with the climatic shift from “greenhouse” to “icehouse” conditions ~30My ago
- Examine the stability of the permanent Antarctic ice sheet over its ~20My history

Glacial Retreat in Antarctica and Deglaciation of the Earth System (GRADES)

- GRADES will investigate the state and stability of the Antarctic ice sheet. A key objective is to improve predictions of Antarctica's contribution to global mean sea level rise.
- The West Antarctic Ice Sheet (WAIS) may be unstable because its base lies on rock below sea level. Measurements from satellites show that there is currently a substantial imbalance in part of the WAIS, which is contributing significantly to sea-level rise. BAS and the University of Texas, supported by US logistics, have already completed an airborne radio-echo sounding survey of approximately one third of the WAIS, covering the region where the most rapid change is taking place. GRADES will study further this important area to better predict how the WAIS contributes to sea level rise.
- GRADES will also develop ice-sheet models and test them using newly acquired ice-sheet histories. We use satellite data, reconstructions of past states of the ice sheet, and new data assimilation techniques to learn more about how ice sheets develop and evolve.

Objectives

- Understand the role of ice sheet disintegration in global climate change
- Assess what is causing the current imbalance in the WAIS
- Search for evidence of previous periods of rapid ice loss in the WAIS
- Determine the contribution of the WAIS to future sea level change

Aurora Pictures


Splitting – Upwind Scheme

Using the splitting upwind method the forward finite difference for $(\partial f_{i,j}^{n,n}/\partial t)$, where ^{n,n}, denotes n^{th} timestep, in space i and velocity space j :

$$\frac{\partial f_{i,j}^{n,n}}{\partial t} = -v_j \left(\frac{f_{(i+m),j}^{n,n} - f_{i+m-1,j}^{n,n}}{\Delta z} \right) \quad (4)$$

where m=(1-s)/2, s=sign(v_j). Integrating for $\Delta t/2$:

$$f_{i,j}^{n+1/2,n} = f_{i,j}^{n,n} + \frac{\Delta t}{2} \frac{\partial f_{i,j}^{n,n}}{\partial t} \quad (5)$$

$$\frac{\partial f_{i,j}^{n+1/2,n}}{\partial t} = -\frac{q_\alpha}{m_\alpha} E_i^{n+1/2} \left(\frac{f_{i,(j+m)}^{n+1/2,n} - f_{i,j+m-1}^{n+1/2,n}}{\Delta v_z} \right) \quad (6)$$

where m=(1-s)/2, s=sign($\frac{q_\alpha}{m_\alpha} E_i^{n+1/2}$). Integrating for Δt:

$$f_{i,j}^{n+1/2,n+1} = f_{i,j}^{n+1/2,n} + \Delta t \frac{\partial f_{i,j}^{n+1/2,n}}{\partial t} \quad (7)$$

$$\frac{\partial f_{i,j}^{n+1/2,n+1}}{\partial t} = -v_j \left(\frac{f_{(i+m),j}^{n+1/2,n+1} - f_{i+m-1,j}^{n+1/2,n+1}}{\Delta z} \right) \quad (8)$$

where m=(1-s)/2, s=sign(v_j). Integrating for $\Delta t/2$:

$$f_{i,j}^{n+1,n+1} = f_{i,j}^{n+1/2,n+1} + \frac{\Delta t}{2} \frac{\partial f_{i,j}^{n+1/2,n+1}}{\partial t} \quad (9)$$

In-pairs integration method [*Horne and Freeman*, 2001].

$$\begin{aligned} n_\alpha(z,t) &= \int_{-\infty}^{\infty} f_\alpha(z, v_z, t) dv_z \\ &= \sum_{i=-N_v}^{N_v-1} \frac{1}{2} \left[f_\alpha(z,i,t) + f_\alpha(z,i+1,t) \right] \Delta v_z (8) \end{aligned}$$

$$\begin{aligned} n_\alpha(z,t) &= \left[\frac{1}{2} f_\alpha(z,-N_v,t) + \frac{1}{2} f_\alpha(z,N_v,t) \right] \Delta v_z \\ &+ \left[\sum_{i=-N_v}^{0} \left[f_\alpha(z,i,t) + f_\alpha(z,-i,t) \right] \right] \Delta v_z \quad (9) \end{aligned}$$

Electron Full Distribution Function

- Dx = Lmin/30 = 0.96 (m) = 0.24 debye length
- Lx = 2 Lmax = 2533.5 (m) = 635 debye lengths
- Dve = 0.0133 U thermal
- Drift Velocity - V_{de} = 1.2 x $(2T/m)^{1/2}$
- M_i=1836 m_e, T_i=1 eV, T_e = 2 eV
- n_i=n_e = 7 x 10^6 /m^3
- Grid: N_z = 2643, N_{ve} = 1203, N_{vi} = 307

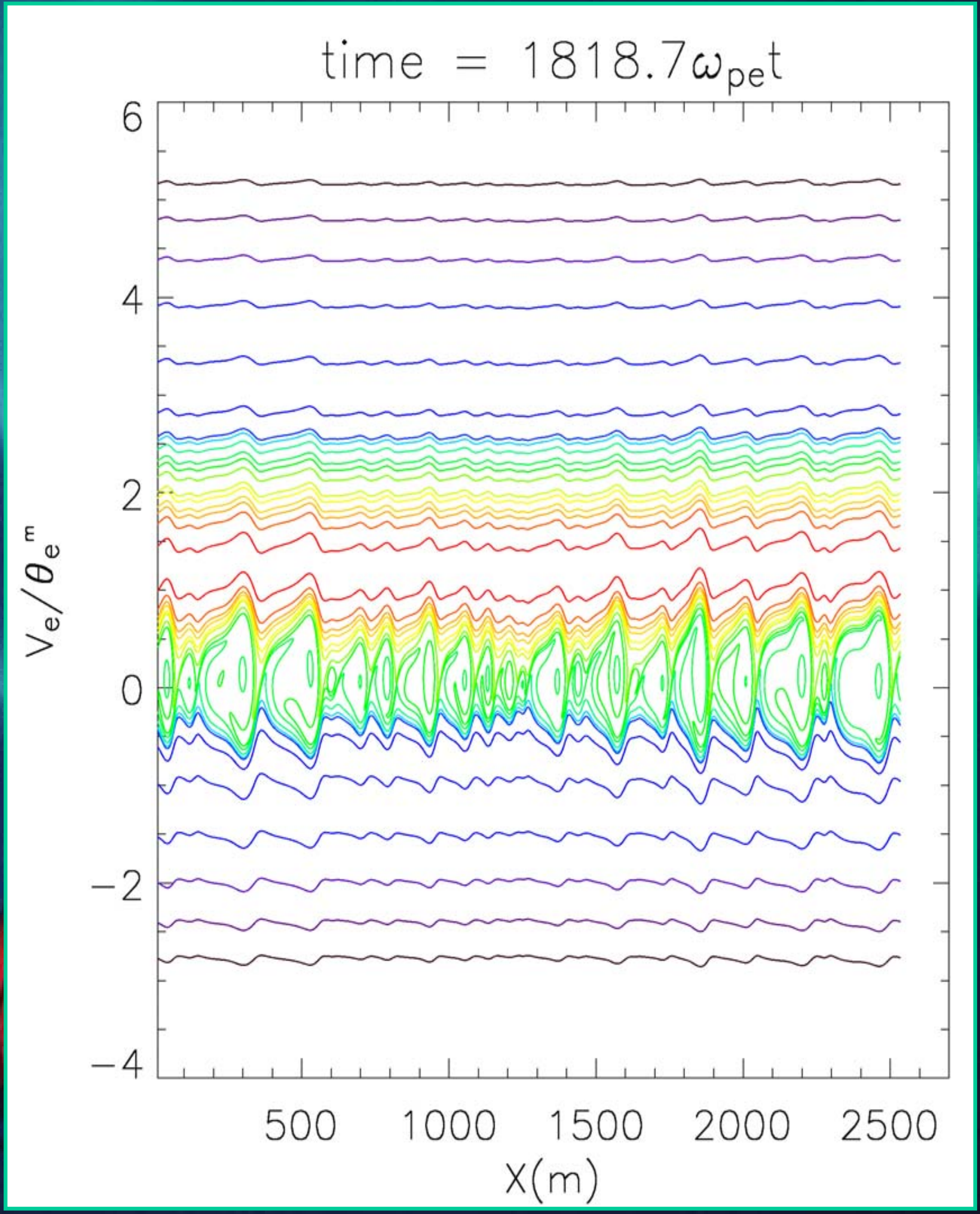

Electric Field Spectra

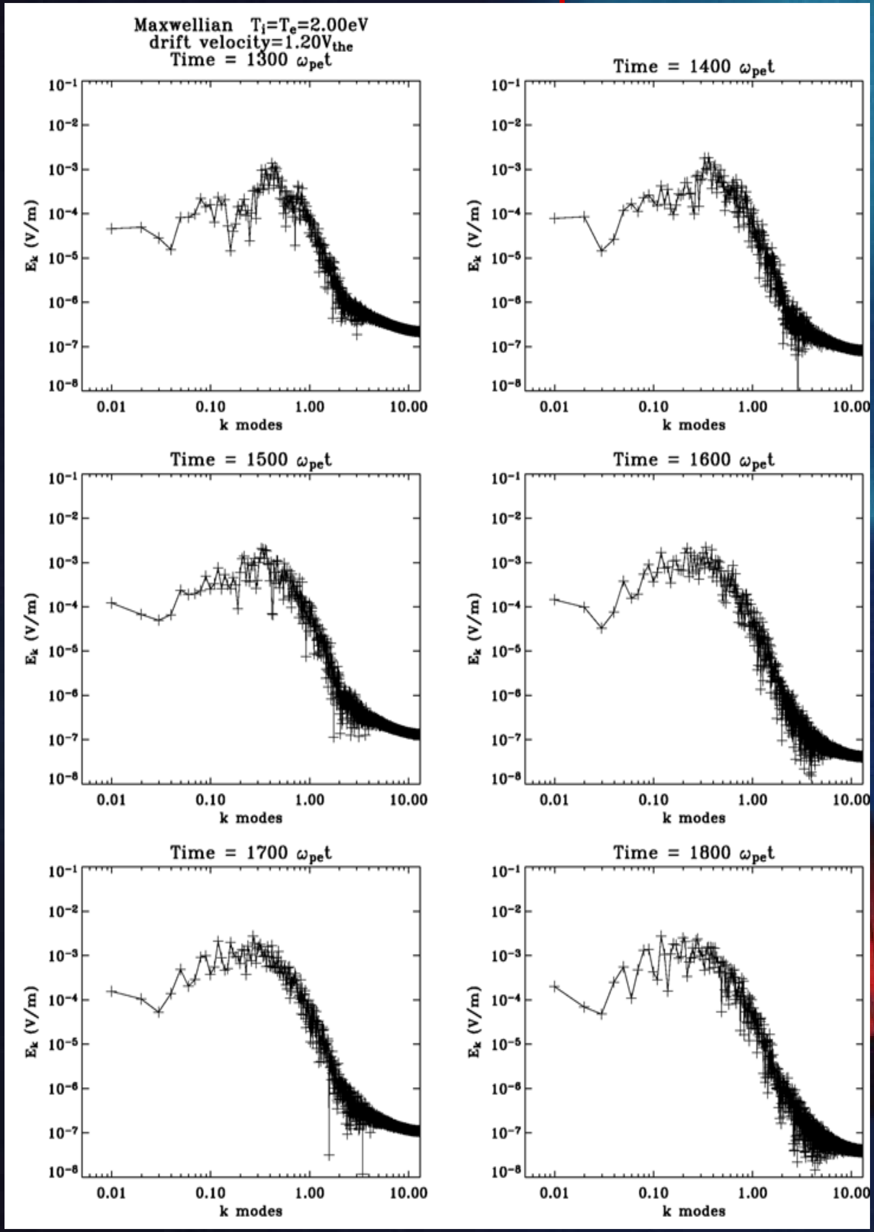

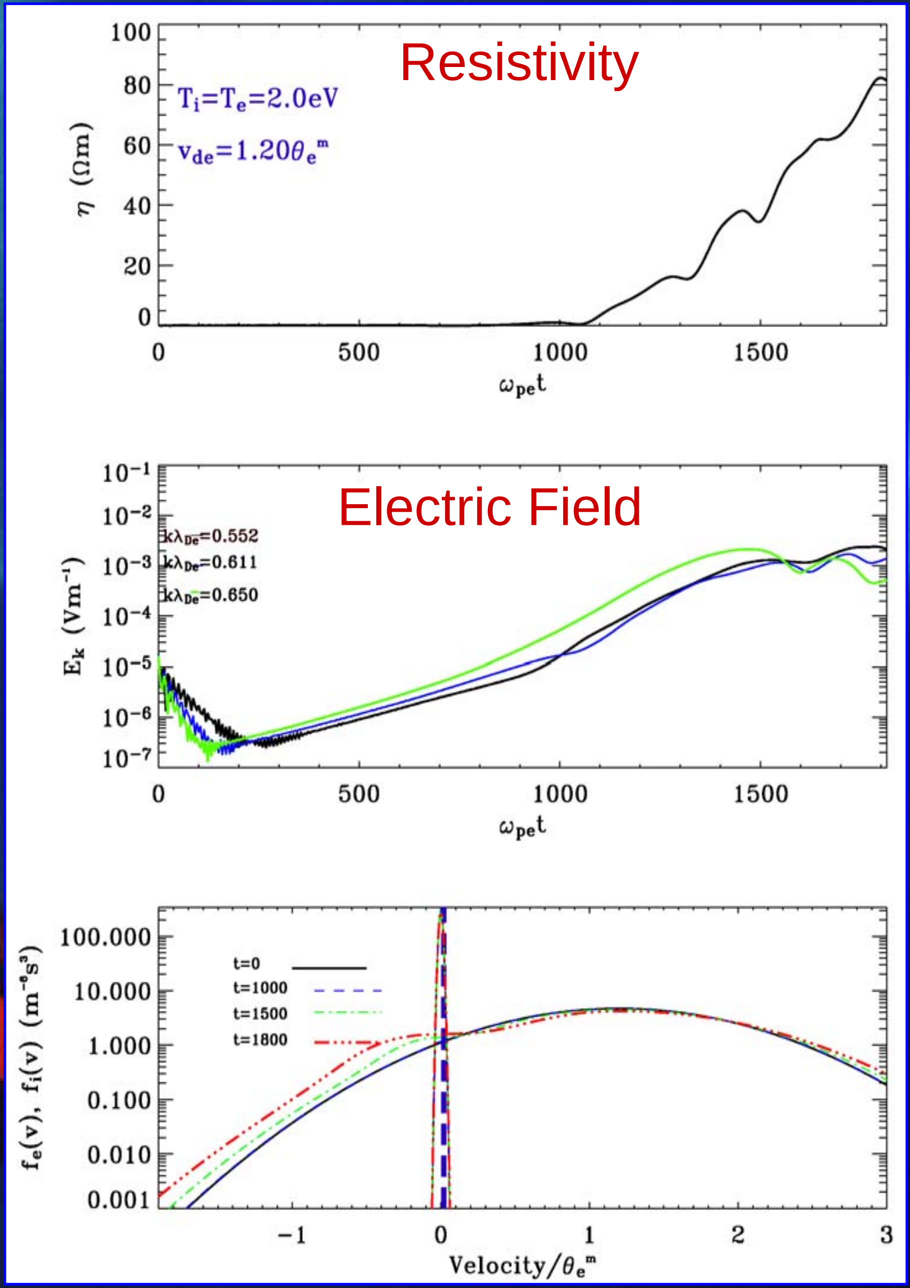

Resistivity order of magnitude

$$R_m = \frac{vL}{\eta}$$

Magnetic Reynolds Number

Solar Corona : $R_m = 10^8$ $\eta = 0.12\ \Omega m$

Earth's Magnetosphere $R_m = 10^{11}$ $\eta = 0.0009\ \Omega m$

Sagdeev Formula

$$\eta = \frac{\alpha \omega_{pi}}{\omega_{pe}^2 \varepsilon_o} \frac{v_{de}}{c_s} \frac{T_e}{T_i} \quad \alpha \approx 0.01$$

- **$V_{de} = 1.2 \times (2T/m)^{1/2}$**
- **$M_i = 1836\ m_e$, $T_i = 1$ eV, $T_e = 2$ eV**
- **$\eta = 16200\ \Omega m$**

Classical Spitzer resistivity

$$\eta_{classical} = \frac{1}{\omega_{pe}^2 \varepsilon_o} \nu_{ei} = \frac{1}{\omega_{pe}^2 \varepsilon_o} 6.2 \times 10^{-5} \frac{n_e}{T_e^{3/2}}$$

$T_e = 2$ eV , $n_e = 7 \times 10^6$ /m^3

$\eta = 6.2\ 10^{-4}\ \Omega m$

Why study Ion-Acoustic Waves?

- Previous analytical estimates and simulations of the resistivity due to current-driven ion-acoustic waves have concentrated on the regime where electron temperature far exceeds ion temperature. Not always the case in space plasmas.
- A Maxwellian plasma with similar electron and ion temperatures, needs a large current to excite unstable ion-acoustic waves. Ion-acoustic waves are measured in many regions of space plasma, and in laboratory plasma experiments indicates the need to study them in more detail for a range of plasma parameters.

Ion-Acoustic Waves in Space Plasmas

- For $T_e \sim T_i$ damped

  Both Distribution Functions have negative gradient

$$k\lambda_{De} << 1 \qquad \omega_r \approx kc_s$$

- For T_e » T_i propagate

$$k\lambda_{De} << 1 \qquad \omega_r \approx kc_s \qquad c_s = \left[k_B\left(T_e + 3T_i\right)/m_i\right]^{1/2}$$

$$k\lambda_{De} > 1 \qquad \omega_r \approx \omega_{pi}\left(1 + 3k^2\lambda_{Di}^2\right)^{1/2}$$

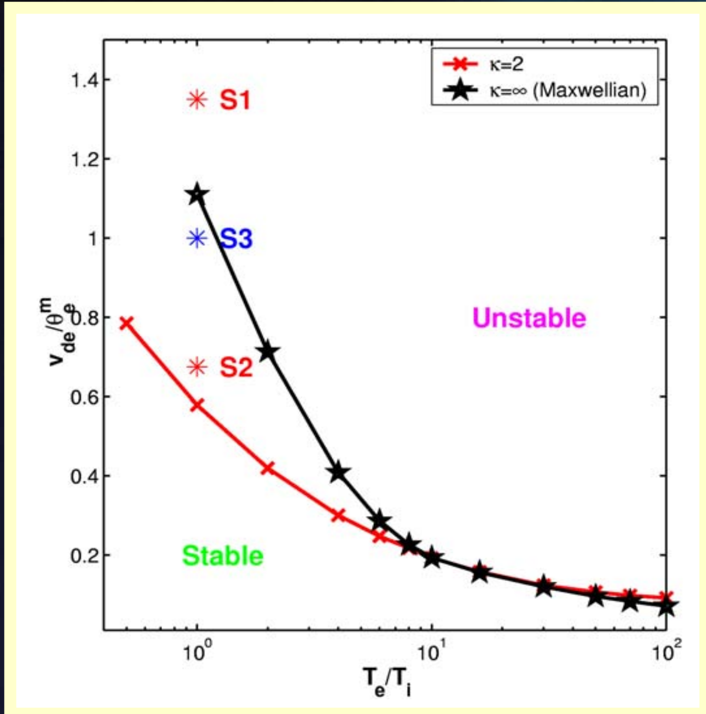

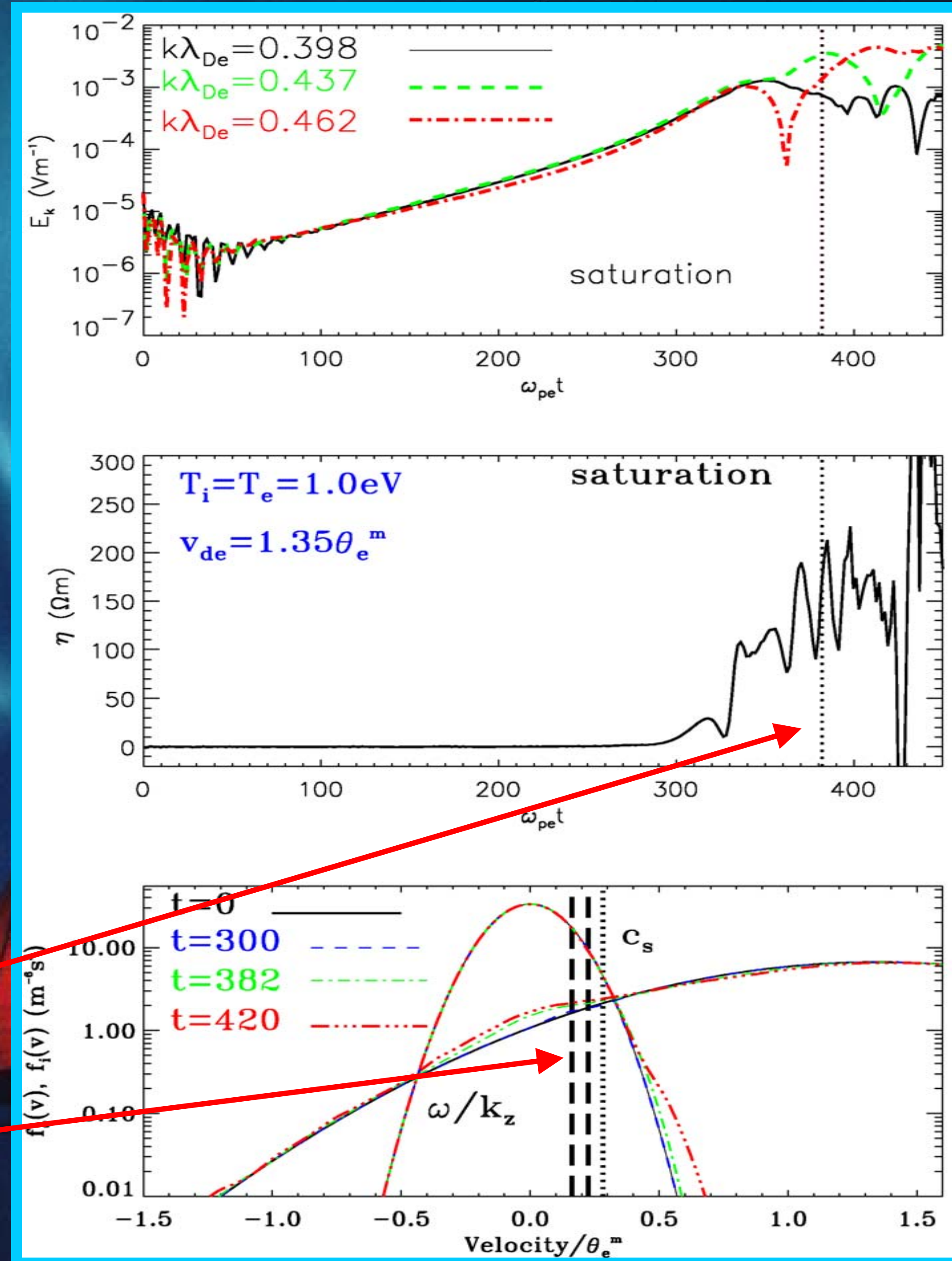

Maxwellian S1

Resistivity at saturation

~ 150 Ohm m

Quasi-linear saturation

Plateau Formation

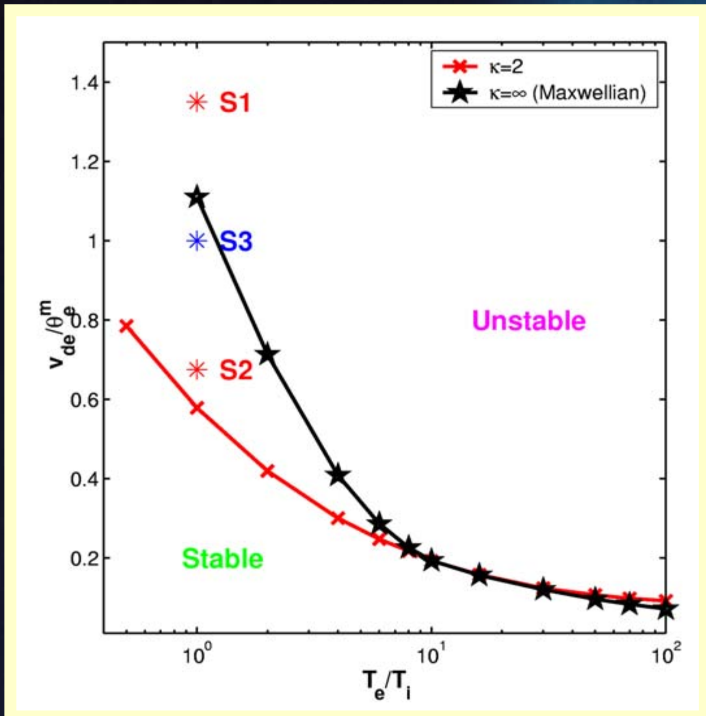

Lorentzian S2
Resistivity at
saturation ~ 20 Ohm
m
Quasi-linear
saturation
Plateau Formation

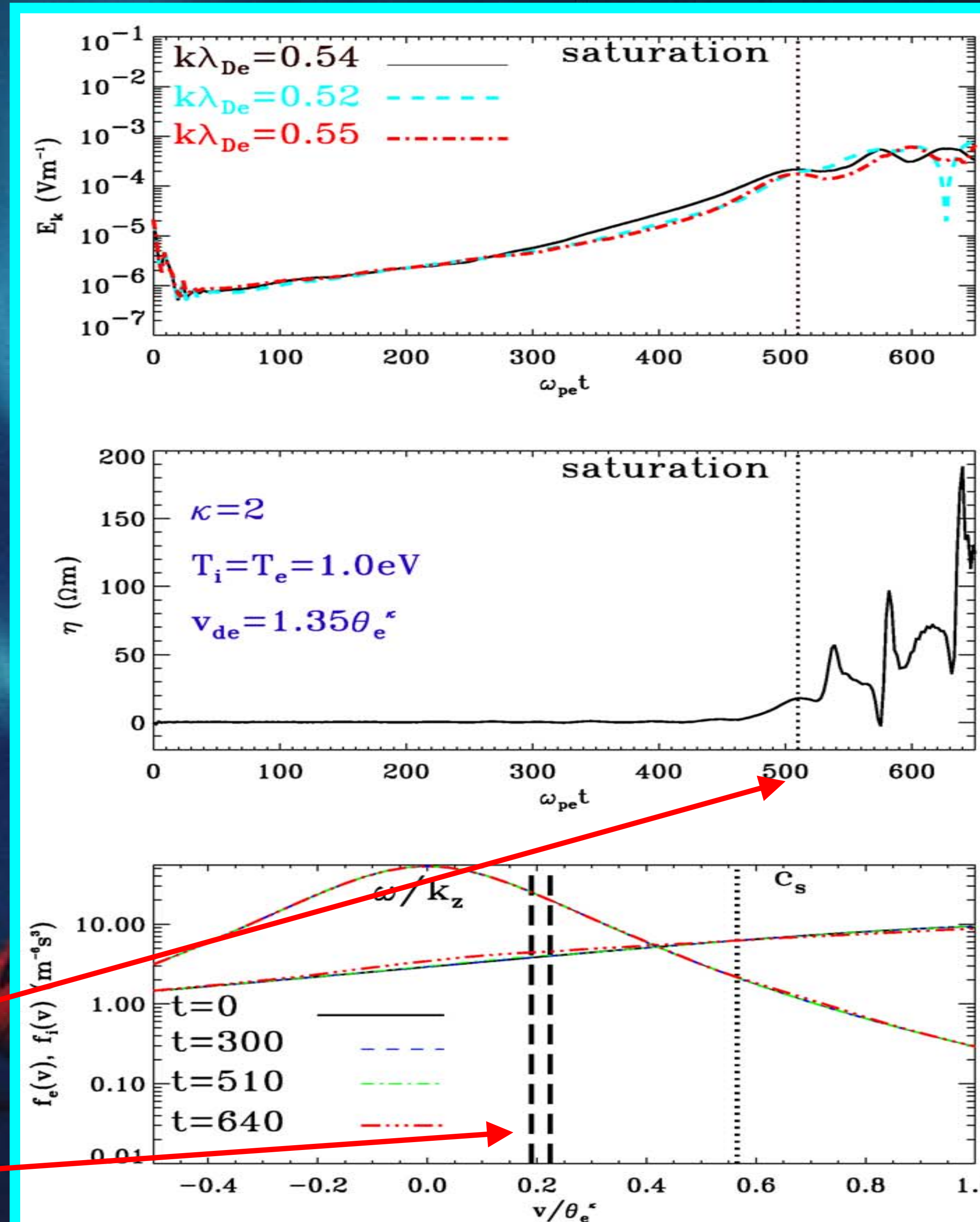

$\kappa = 2$

$T_e/T_i = 1.0$

$M_i/M_e = 25$

$V_{de} = 1.2 \times \theta_e$

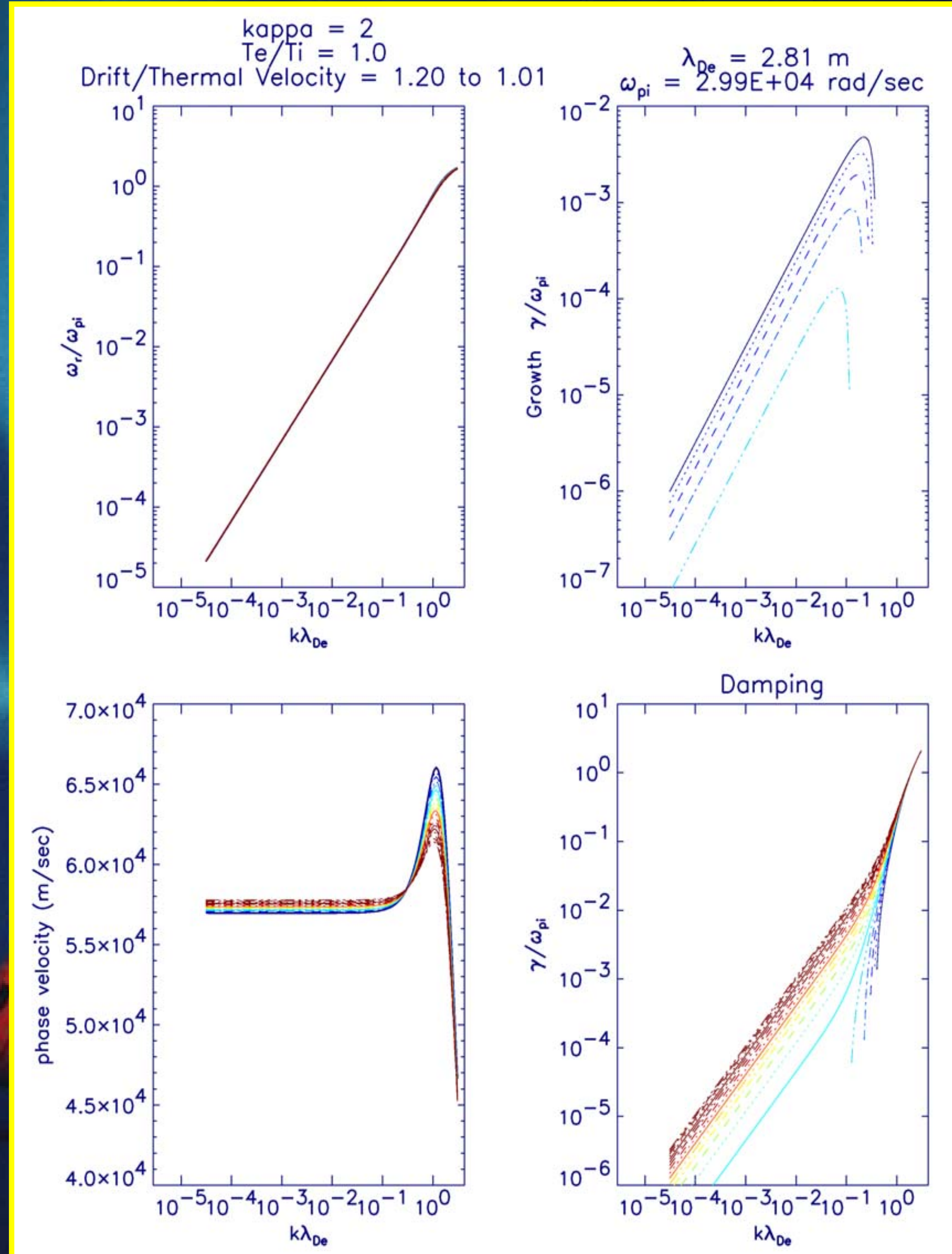

Modified Plasma Dispersion Function and Derivative

$$Z_\kappa^* = -\frac{(\kappa - 1/2)}{2\kappa^{3/2}} \frac{\kappa!}{(2\kappa)!} \sum_{l=0}^{\kappa} \frac{(\kappa+l)!}{l!} i^{\kappa-l} \left(\frac{2}{\left(\xi/\sqrt{\kappa}\right) + i} \right)^{\kappa+1-l}$$

$$\frac{dZ_\kappa^*(\xi)}{d\xi} = -2\left(1 - \frac{1}{4\kappa^2}\right) - 2\left(\frac{\kappa - 1/2}{\kappa}\right)\left(\frac{\kappa+1}{\kappa}\right)^{3/2} \times \xi \quad Z_{\kappa+1}^*(\xi) \left[\left(\frac{\kappa+1}{\kappa}\right)^{1/2} \xi \right]$$

Previous analytical work

- **Analytical estimates of the resistivity due to ion-acoustic waves:**
  - *Sagdeev [1967]:*

$$\eta = \frac{\alpha \omega_{pi}}{\omega_{pe}^2 \varepsilon_o} \frac{v_{de}}{c_s} \frac{T_e}{T_i} \quad \text{where } \alpha \approx 0.01$$

  - *Labelle and Treumann [1988]:*

$$\eta = \frac{1}{\omega_{pe} \varepsilon_o} \frac{W_E}{n k_B T_e}$$

- **Both estimates assume $T_e \gg T_i$ which is not the case for most space plasma regions of interest (e.g. magnetopause).**

STAFF overplotted |B|

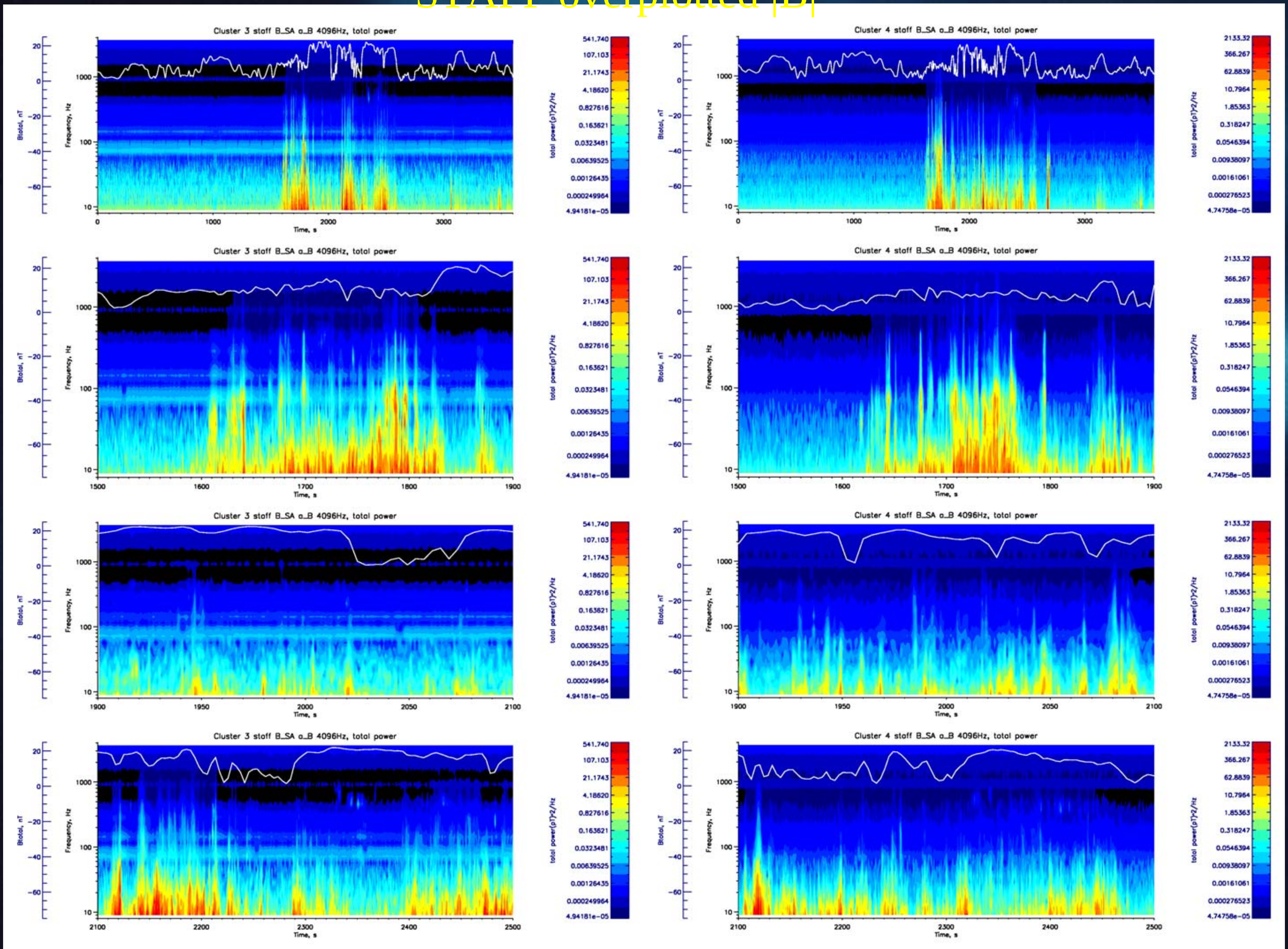

STAFF overplotted |B|

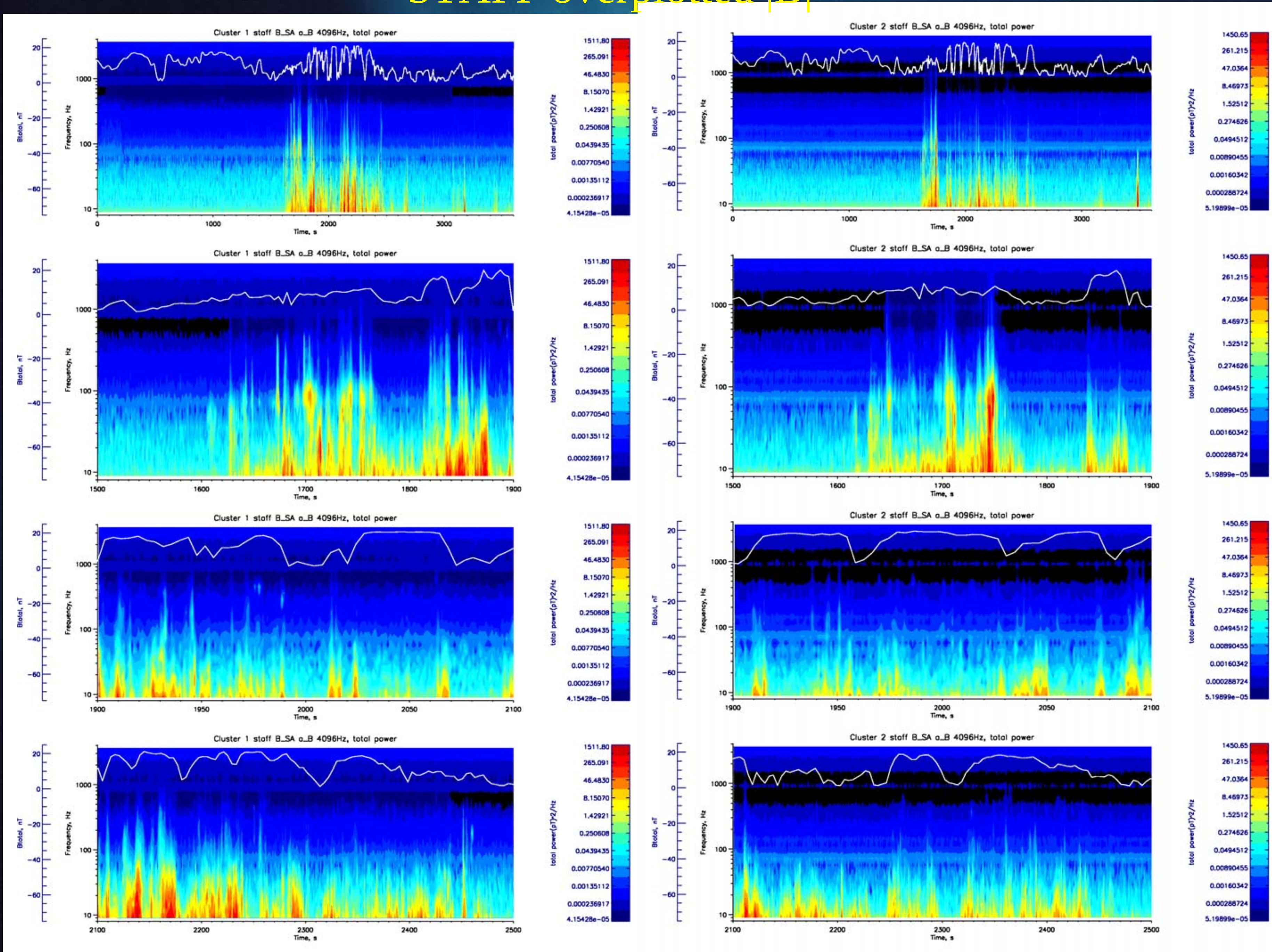

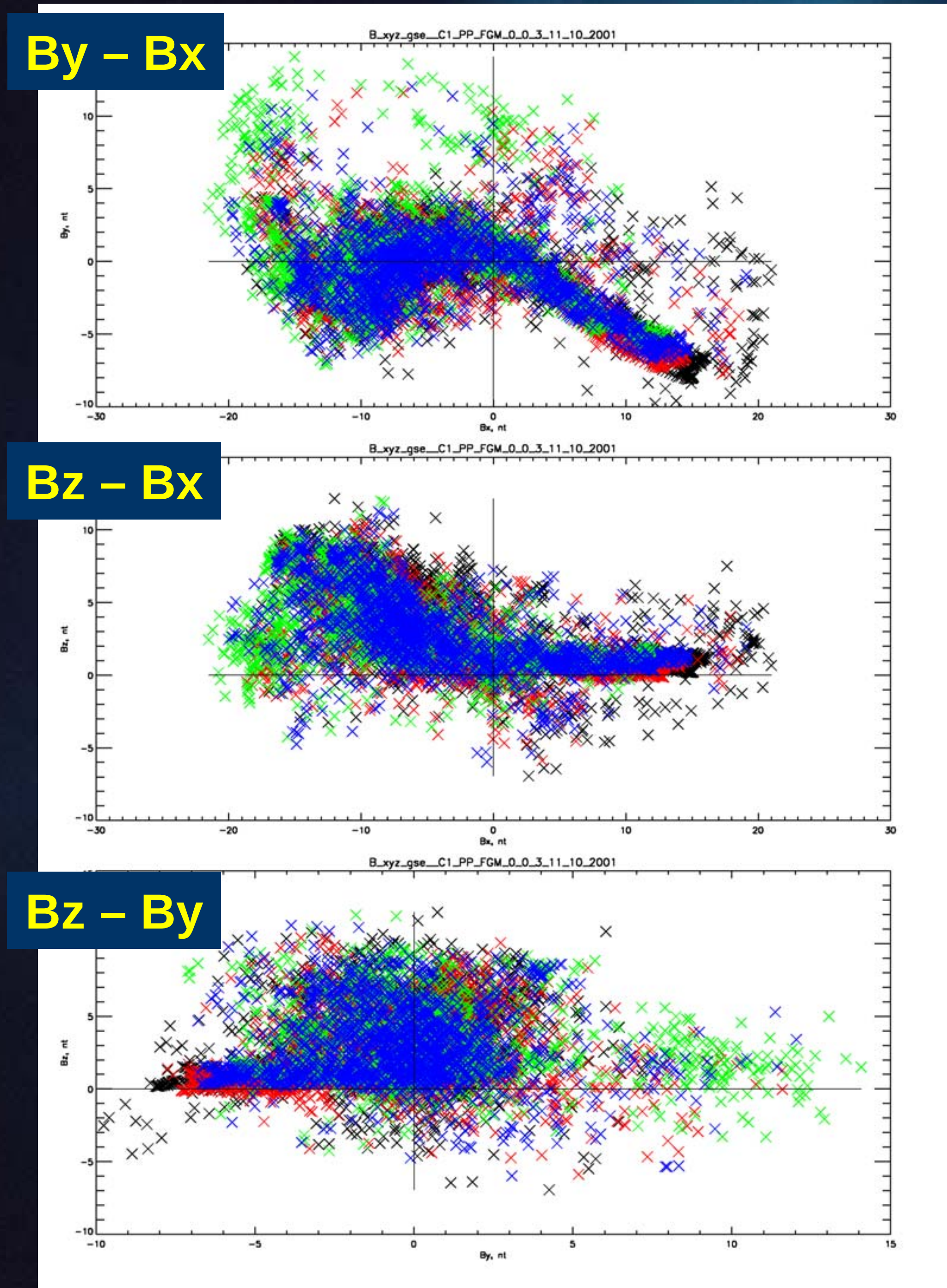

11/10/2001 – 0300

- **Scatter Diagram of Magnetic field**
- **By – Bx**
- **Bz – Bx**
- **Bz – By**
- **Regime A+B+C (1500-2500)**
- **The four spacecraft follow a similar locus in magnetic field phase space, suggesting that the current sheet structure is relatively stable**
- **Also evidence of some transient departures.**

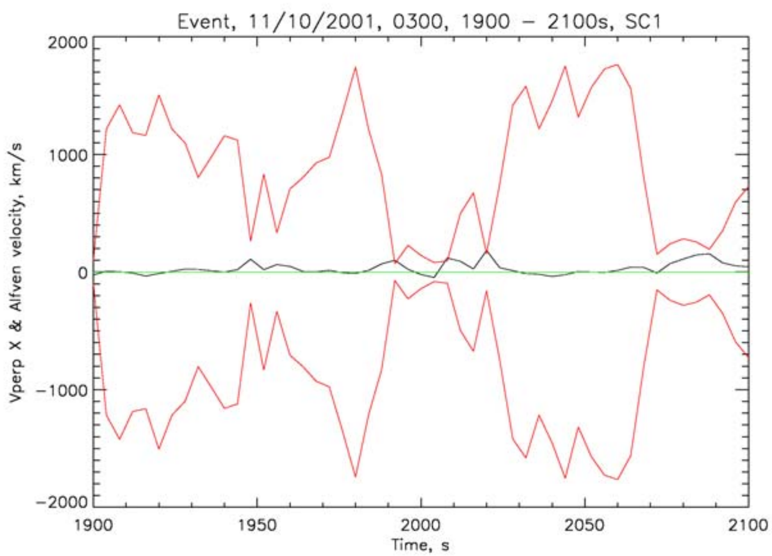
Event, 11/10/2001, 0300, 1900 – 2100s, SC1
Vperp X & Alfven velocity, km/s
Time, s

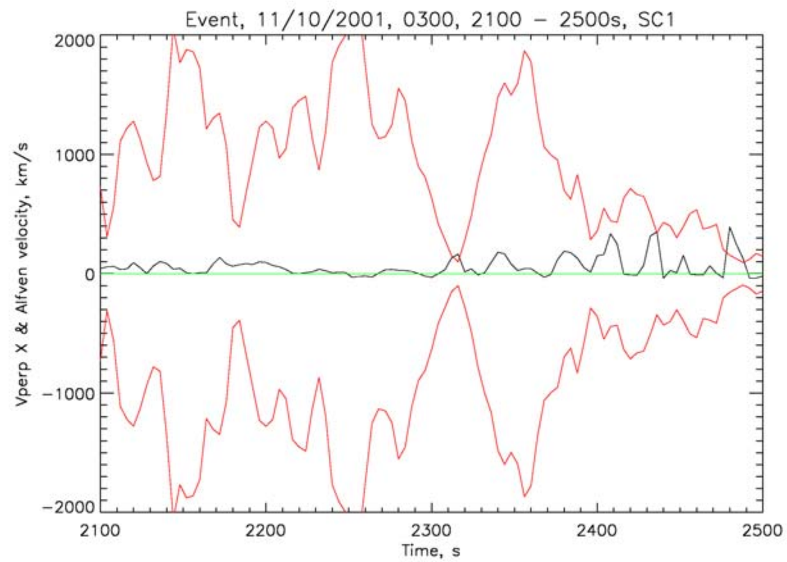
Event, 11/10/2001, 0300, 2100 – 2500s, SC1
Vperp X & Alfven velocity, km/s
Time, s

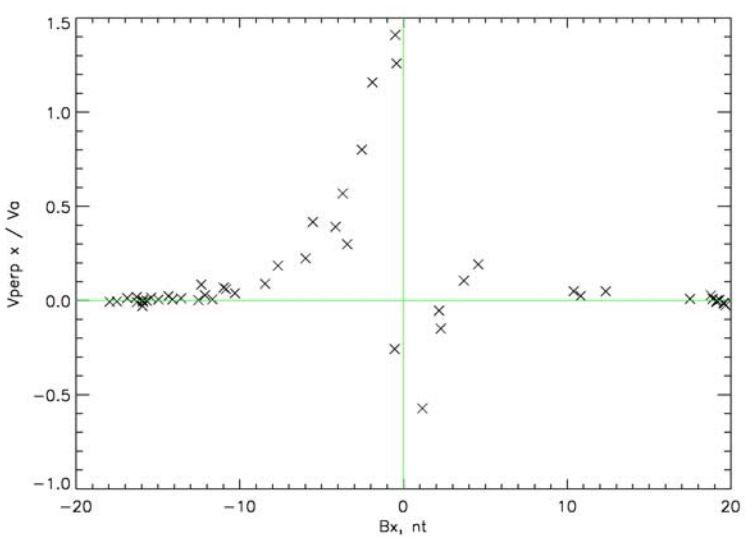
Vperp x / Va
Bx, nt

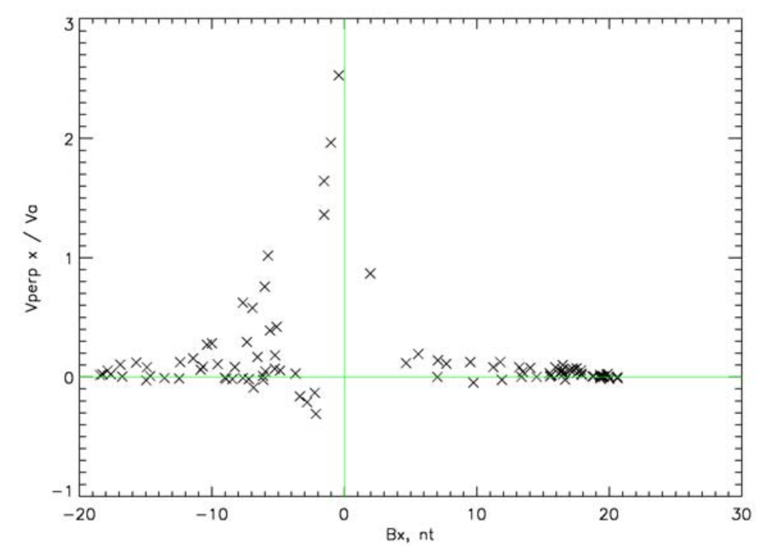
Vperp x / Va
Bx, nt

Wave Power in terms of |B|, Regime B and C